

Live while the DNA lasts. The role of autophagy in DNA loss and survival of diploid yeast cells during chronological aging

Tuguldur Enkhbaatar¹, Marek Skoneczny¹, Karolina Stępień², Mateusz Mołoń³,
Adrianna Skoneczna¹

¹Institute of Biochemistry and Biophysics, Polish Academy of Sciences, Warsaw 02-106, Poland

²Institute of Medical Sciences, Rzeszów University, Rzeszów 35-959, Poland

³Institute of Biology, Rzeszów University, Rzeszów 35-601, Poland

Correspondence to: Adrianna Skoneczna; email: ada@ibb.waw.pl

Keywords: aging, genome instability, lifespan, autophagy, double-strand breaks

Received: June 13, 2023

Accepted: September 6, 2023

Published: October 9, 2023

Copyright: © 2023 Enkhbaatar et al. This is an open access article distributed under the terms of the [Creative Commons Attribution License](https://creativecommons.org/licenses/by/3.0/) (CC BY 3.0), which permits unrestricted use, distribution, and reproduction in any medium, provided the original author and source are credited.

ABSTRACT

Aging is inevitable and affects all cell types, thus yeast cells are often used as a model in aging studies. There are two approaches to studying aging in yeast: replicative aging, which describes the proliferative potential of cells, and chronological aging, which is used for studying post-mitotic cells. While analyzing the chronological lifespan (CLS) of diploid *Saccharomyces cerevisiae* cells, we discovered a remarkable phenomenon: ploidy reduction during aging progression. To uncover the mechanism behind this unusual process we used yeast strains undergoing a CLS assay, looking for various aging parameters. Cell mortality, regrowth ability, autophagy induction and cellular DNA content measurements indicated that during the CLS assay, dying cells lost their DNA, and only diploids survived. We demonstrated that autophagy was responsible for the gradual loss of DNA. The nucleophagy marker activation at the start of the CLS experiment correlated with the significant drop in cell viability. The activation of piecemeal microautophagy of nucleus (PMN) markers appeared to accompany the chronological aging process until the end. Our findings emphasize the significance of maintaining at least one intact copy of the genome for the survival of post-mitotic diploid cells. During chronological aging, cellular components, including DNA, are exposed to increasing stress, leading to DNA damage and fragmentation in aging cells. We propose that PMN-dependent clearance of damaged DNA from the nucleus helps prevent genome rearrangements. However, as long as one copy of the genome can be rebuilt, cells can still survive.

INTRODUCTION

Aging is an inevitable process that affects all organisms, regardless of whether they are unicellular or part of higher-organized multicellular organisms, such as mammals. This process is of great interest to researchers, as each new study in this area brings hope for discovering ways to delay aging. Since aging is a universal cellular problem, it is understandable that yeast cells are commonly used as a model for studying aging (reviewed in [1, 2]). Two main approaches to studying aging in yeast cells are used [3, 4], and these

approaches yield different lifespan parameters [5]. Replicative lifespan (RLS) refers to the number of mitotic divisions a given mother cell can undergo before reaching senescence and death [6]. Senescence is the period after the last division during which the cell is still alive [5]. Chronological lifespan (CLS) refers to the length of time a post-mitotic cell population (in yeast, stationary phase culture) can still give rise to progeny [7].

We have learned a great deal about the factors that influence aging, some of which are related to mutations

in the genome. It is well known that RLS is strongly influenced by signal transduction pathways' efficiency (such as TOR [8] or PKA-dependent pathways [9]), chromatin remodeling ([10], with sirtuins [11–13] playing a widely explored role), DNA damage response pathways' effectiveness in preventing genome instability and ensuring proper DNA segregation [14, 15], metabolic potential of the cells [16–19], and cell polarity and size [20–22]. A growing body of evidence suggests that CLS depends on similar factors. Signal transduction pathways, chromatin remodeling, and genome maintenance [7, 11, 23, 24], proper stress response [25], metabolic potential of the cells [26–30], and cell wall content, which determines stress resistance and cell size [31], are all crucial for CLS. Yeast cells lacking mitochondrial or autophagy-related genes in their genomes consistently exhibit a shortened CLS [32]. Lifespan also depends on extracellular factors; for example, glucose limitations cause lifespan extension [33]. This effect, known as caloric restriction, can be nullified by methionine supplementation [34]. Similarly, mutations that affect signal transduction pathways can lead to improper sensing of environmental resources [35], resulting in similar outcomes. However, despite identifying some mutations in the cellular background or environmental conditions that might influence aging speed, we still do not know the real factor that limits/determines cell lifespan.

In our previous research, we investigated whether disturbances in the G1/S phase transition, such as a delay in the START point of replication due to reduced levels of proteins required to initiate this process, could affect the CLS of yeast. Using diploid *Saccharomyces cerevisiae* strains heterozygous for genes encoding subunits of the origin recognition complex (*ORC1* to *ORC6*), we found that reducing the levels of any of the Orc1–6 proteins resulted in a significant increase in the budding lifespan and delayed average chronological aging, likely due to the delay in the cell cycle and subsequent extension of the doubling time [36]. During this study, we observed unexpected phenotypes of *S. cerevisiae* cells. At some stage in CLS, diploid cells reduced their DNA content to the level typical of haploid cells. We ruled out sporulation as the cause of haploidization, but how it occurs remained unanswered. In this paper, we attempted to address this issue. We demonstrated that a decrease in DNA content is accompanied by activating two autophagy pathways: nucleophagy and PMN. We also found that cells require at least one intact genome to survive the CLS experiment since cells with less than this minimum were dying, both haploids and diploids. In other words, cells live as long as their genome is restorable, and full DNA content is the limit of life.

RESULTS

Cells losing their DNA during CLS

The data we obtained earlier drew our attention to the fact that diploid yeast cells analyzed during CLS had a reduced DNA content [36]. This phenomenon was observed not only in cells of six heterozygous strains with decreased expression of respective ORC complex subunits but also in the control strain, in all biological repetitions. The result was surprising but repetitive, and certainly worth further investigation. To validate this observation, we repeated the CLS experiment once more using a diploid wild-type strain, and we observed the same result (Figure 1A–1C; see also Supplementary Figure 1 for the controls). During the CLS assay, cell viability significantly decreased, and with time, diploid *S. cerevisiae* cells reduced their ploidy to the typical haploid level while their size remained relatively constant.

We considered several hypotheses to explain the ploidy reduction observed during CLS, including (1) sporulation, (2) DNA degradation, and (3) gradual loss of one copy of the genome. It is also possible that the apparent ploidy reduction is due to DNA condensation, which reduces its saturation with propidium iodide (PI), resulting in no change in the DNA content of aging cells. However, we excluded the hypothesis of sporulation as a source of ploidy reduction based on several arguments. First, a microscopic examination of the strain cultures during the CLS assay revealed no tetrads. Second, spores cannot germinate under nutrient-poor and inaccessible conditions. To verify the hypothesis of DNA degradation as a cause of DNA content reduction, we performed pulse-field gel electrophoresis (PFGE) to analyze the integrity of yeast chromosomes at the beginning and end of the CLS assay (Figure 1D). Our results showed that DNA in the aged cells undergoes fragmentation (Figure 1E). However, the histogram of DNA content we observed in flow cytometry analysis (Figure 1B) did not show DNA debris that should appear as a peak close to the Y-axis. We considered that a substantial part of DNA fragments might be lost during the lengthy preparation of DNA embedded in agarose plugs before PFGE analysis. With these conflicting results, we could not determine whether the gradual loss of DNA or DNA degradation is the source of ploidy reduction during CLS. Nevertheless, we could rule out the possibility that genomic DNA condenses over time, making fluorescent dye intercalation difficult and causing an artificial ploidy shift.

Cells surviving CLS are diploids

As the previous results did not provide a clear answer to the question of the mechanism behind the observed

ploidy shift during CLS of diploid yeast, we took a different approach. We asked what was the ploidy of cells that remained alive at each time point of the CLS experiment. To answer this question, we sampled the aging cells at the specific days of the CLS experiment and inoculated them into fresh medium. Then we compared the DNA content of the aging cells with the DNA content of regrown cells from the same day (see Materials and Methods for more details). Figure 2A, 2B

display the results of this experiment, which showed that only diploid cells could regrow.

A single copy of the genome allows surviving CLS of both haploids and diploids

Since only diploids survived in the aging population, we investigated whether the percentage of diploid cells observed in the aging population on a given day

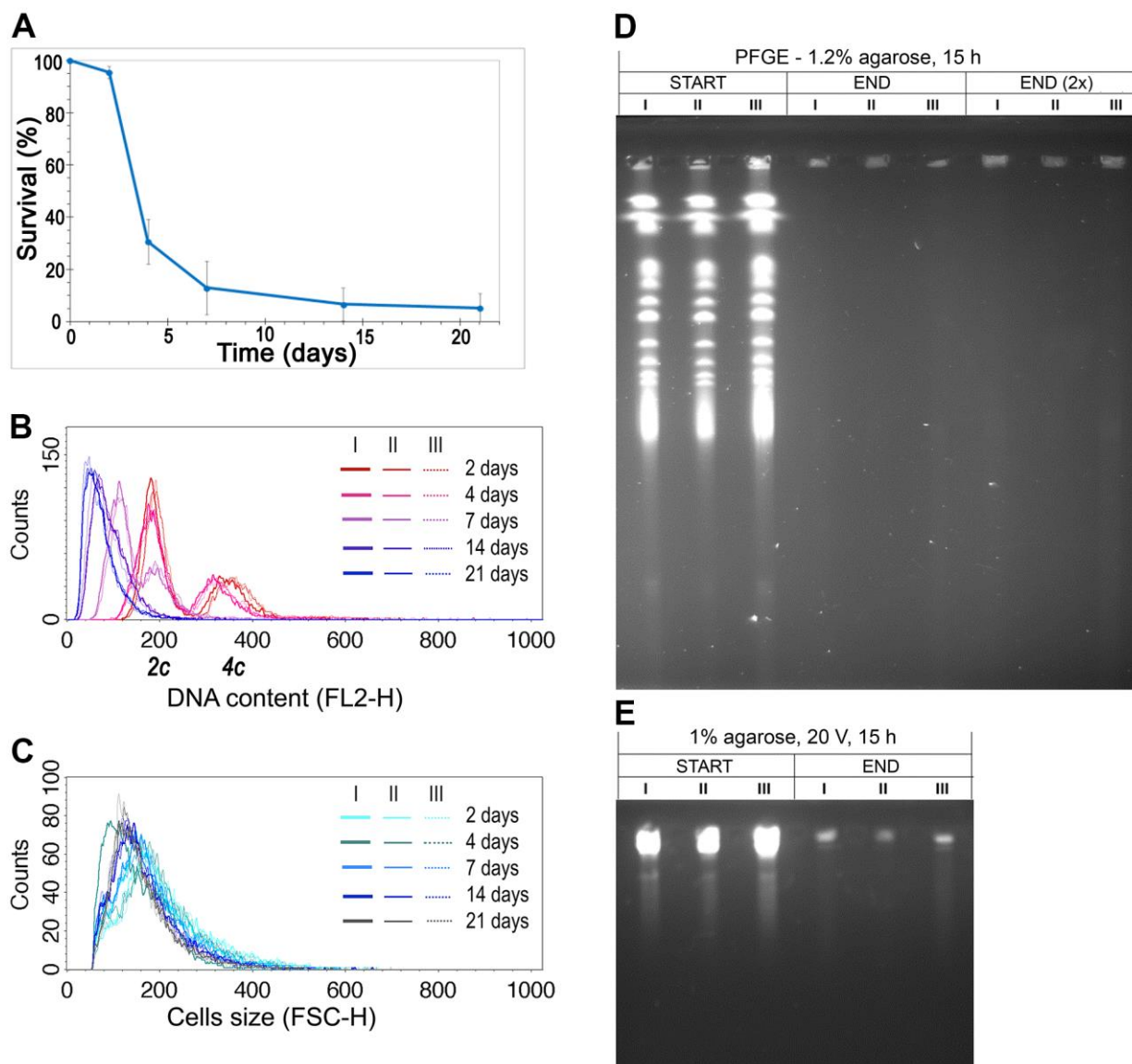


Figure 1. DNA content reduction is associated with the CLS of the diploid yeast. (A) CLS of diploid (BY4743) wild-type strain. The mean from three biological repetitions is shown. Bars indicate standard deviations. (B) Changes in the DNA content of the WT (BY4743) strain during CLS were assessed by flow cytometry of propidium iodide-stained cells. Three biological repetitions labeled I, II, and III are shown. 2c, two DNA content (DNA content typical for diploid in G1 phase), 4c, four DNA content (DNA content typical for diploid in G2 phase of the cell cycle) (C) The cell size changes observed in the WT (BY4743) strain during CLS assessed by flow cytometry. Three biological repetitions are shown. (D, E) The genome integrity of yeast cells, subject to CLS, at the 2nd day (START) and 21st day (END) of the experiment. Chromosome integrity was assessed by PFGE (D) and classical agarose electrophoresis (E). Three biological repetitions were analyzed. END (2×), for better DNA visualization, the amount of analyzed sample was doubled.

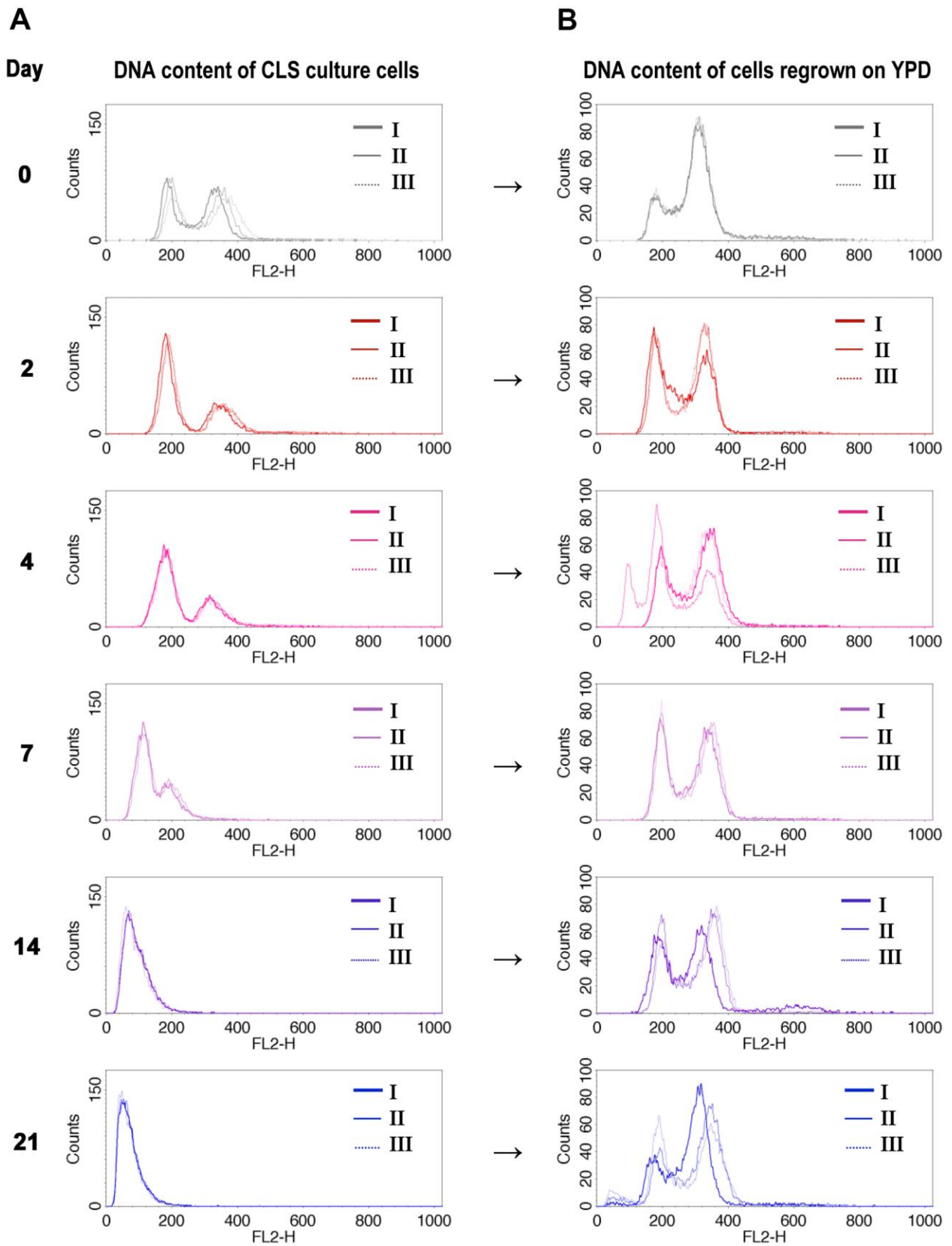


Figure 2. DNA content of cells that survived CLS assay is diploidal. DNA content of wild-type diploid cells (BY4743) during CLS showed ploidy reduction (A), but only diploids (or near-diploids) can survive and start to grow when transferred to the fresh medium (B). The I, II, III labels indicate the biological repetition.

corresponded to the number of cells that remained viable on that day. We gated the population of diploid cells on the (FL2-A SCH) scatter plot graphs obtained during flow cytometry analysis and checked how their proportion changed with time during CLS. As expected, we observed a decreasing percentage of diploid cells in the aging cell population. However, on the 14th and 21st days of the CLS experiment, the numbers of diploid cells observed were very small and did not match the CLS survival results (compare Figures 1A, 3A). We decided to test the correlation between DNA content and cell survival during the CLS assay using the wild-type haploid strain. Figure 3B shows the decreasing percentage of haploid cells accompanying aging of the haploid population. Surprisingly, we observed a higher fraction of cells with haploid DNA content in the last days of the CLS assay of the haploid strain than the fraction of cells with diploid DNA content in the last days of the CLS assay of the diploid strain. This result contradicted the CLS results obtained for haploid and diploid strains (Figure 3C). It remains unclear why aging diploid cells, lacking their typical DNA content (from $2c$ to $4c$), survive better than aging haploid cells with preserved full haploid DNA content (from $1c$ to $2c$).

Is it possible that a single copy of the yeast genome is enough for survival? To investigate this possibility, we changed the gating parameters and repeated the analysis, as shown in Figure 3D. We observed that not all diploids with typical DNA content were viable. After 4 days, 90% of cells had the expected DNA content, but only 30% were alive. After 7 days, only 30% had the expected DNA content, and 10% were alive. However, on the 14th and 21st day, the proportions were reversed: there were practically no diploids in the assayed population, and about 5% of the cells were still alive. These results can be explained by the fact that one copy of the genome, i.e., $1c$, with all essential genes present, is sufficient for a diploid yeast cell to survive. It appears that diploids can rebuild a second genomic copy based on this single copy because the strains that regrew from the aging population displayed the DNA content typical for diploids (from $2c$ to $4c$, Figure 2). These findings suggest that a single copy of the genome can permit the survival of not only haploid but also diploid cells.

This assumption prompted us to reevaluate the flow cytometry data we obtained for the aging cell population during the CLS assay. This time, we compared the DNA content in the whole cell population to the subpopulations gated with respect to different DNA content in the cell. Figure 3E shows the DNA profiles in the subpopulations of aging cells. The systematic decrease of diploids with time was accompanied by an increasing number of cells with lower DNA content. The number of cells with lower than $1c$ DNA content better reflect cell mortality than

those with DNA content lower than $2c$. This result supports the conclusion that $1c$ DNA content permits cell survival during chronological aging.

Autophagy is induced in the aging cells

The longevity of post-mitotic cells depends on cellular processes capable of degrading old components and replacing them with new ones. According to this scenario, amino acid homeostasis, based on amino acid uptake and recycling, mainly via autophagy of mitochondria and other cellular components, is a process that contributes to the maintenance of cellular homeostasis by removing damaged structures (reviewed in [37]). However, damage also affects other molecules. The loss of proteostasis control and subsequent proteotoxic stress is a well-known hallmark of aging [38]. The damage observed during aging affects all types of molecules, including proteins, lipids, and nucleic acids. Since we detected DNA fragmentation and a gradual decrease in DNA content during the CLS assay, we investigated whether autophagy could be used to clear fragmented DNA.

There are two main pathways involved in the degradation of DNA by autophagy in yeast: nucleophagy and piecemeal microautophagy of the nucleus (PMN) [39]. Each pathway requires a specific protein with a receptor-like function. For nucleophagy, this role is played by Atg39, while for PMN, there are two receptors, Nvj1 and Vac8 [39]. In our experiments, we used cells carrying fluorescently tagged Atg39-GFP (YTE20), Nvj1-GFP (YTE18), Vac8-GFP (YTE19), and GFP-Atg8 (YTE17) as a general control of autophagy induction. The Atg8 protein is activated and overproduced in different autophagy pathways, including the Cvt pathway (i.e., cytoplasm-to-vacuole targeting pathway, which uses autophagosomal-like vesicles for selective transport of proteins to the vacuole), nucleophagy, PMN, mitophagy, and pexophagy. Thus, Atg8 serves as the marker for both micro- and macro-autophagy [40]. Autophagy receptor levels increase during autophagy induction [41–43]. Their levels also increase in stressful conditions known to stimulate autophagy, such as starvation, osmotic, oxidative, or proteotoxic stress [44–46].

To assess the level of autophagy induction, we analyzed the cellular level of several fluorescently tagged proteins, selected as autophagy markers, using flow cytometry. This approach facilitates analysis, especially when proteins of interest are anchored to membranes or possess transmembrane domains, which is the case for PMN and nucleophagy markers. Figure 4A–4D show the results of this analysis. We detected an increase in the fluorescent signal for all tested proteins; however, the pattern of detected changes varied. At the beginning of

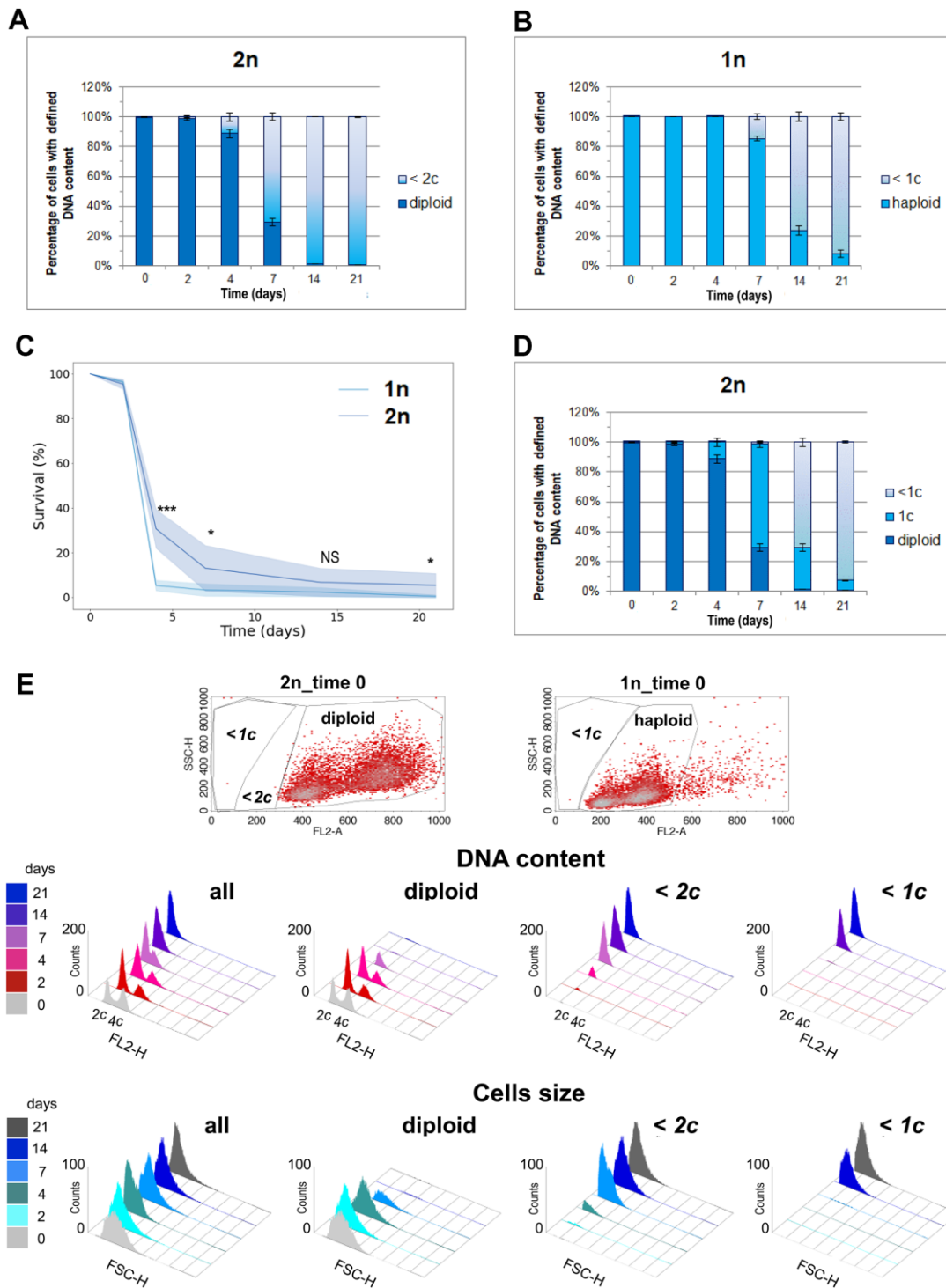


Figure 3. One DNA content permits the survival of the CLS assay. (A) The number of cells with diploid and lower than 2c DNA content was observed at different time points during CLS of the diploid (BY4743) strain. (B) Number of cells with haploid and lower than 1c DNA content observed in different time points during CLS of haploid (BY4741) strain. (C) Comparison of survival rate of diploid (BY4743) versus haploid (BY4741) wild-type strains during CLS assay. The mean from three biological repetitions is shown. Bars indicate standard deviations. Statistical significance was assessed using ANOVA and Dunnett's post hoc test (* $p < 0.05$; *** $p < 0.001$). (D) Number of cells with diploid, 1c, and lower than 1c DNA content observed in different time points during CLS of diploid (BY4743) strain. (A, C, D) The mean from three biological repetitions is shown. Bars indicate standard deviations. (E) Flow cytometry results show changes in the DNA content and cell size during the CLS experiment in the whole cell population and its fractions defined as diploids and cells with DNA contents lower than 2c or 1c. The upper panel shows scatter plots for exponentially grown haploid and diploid strains, which enabled the setting up of gating conditions to determine specific subpopulations.

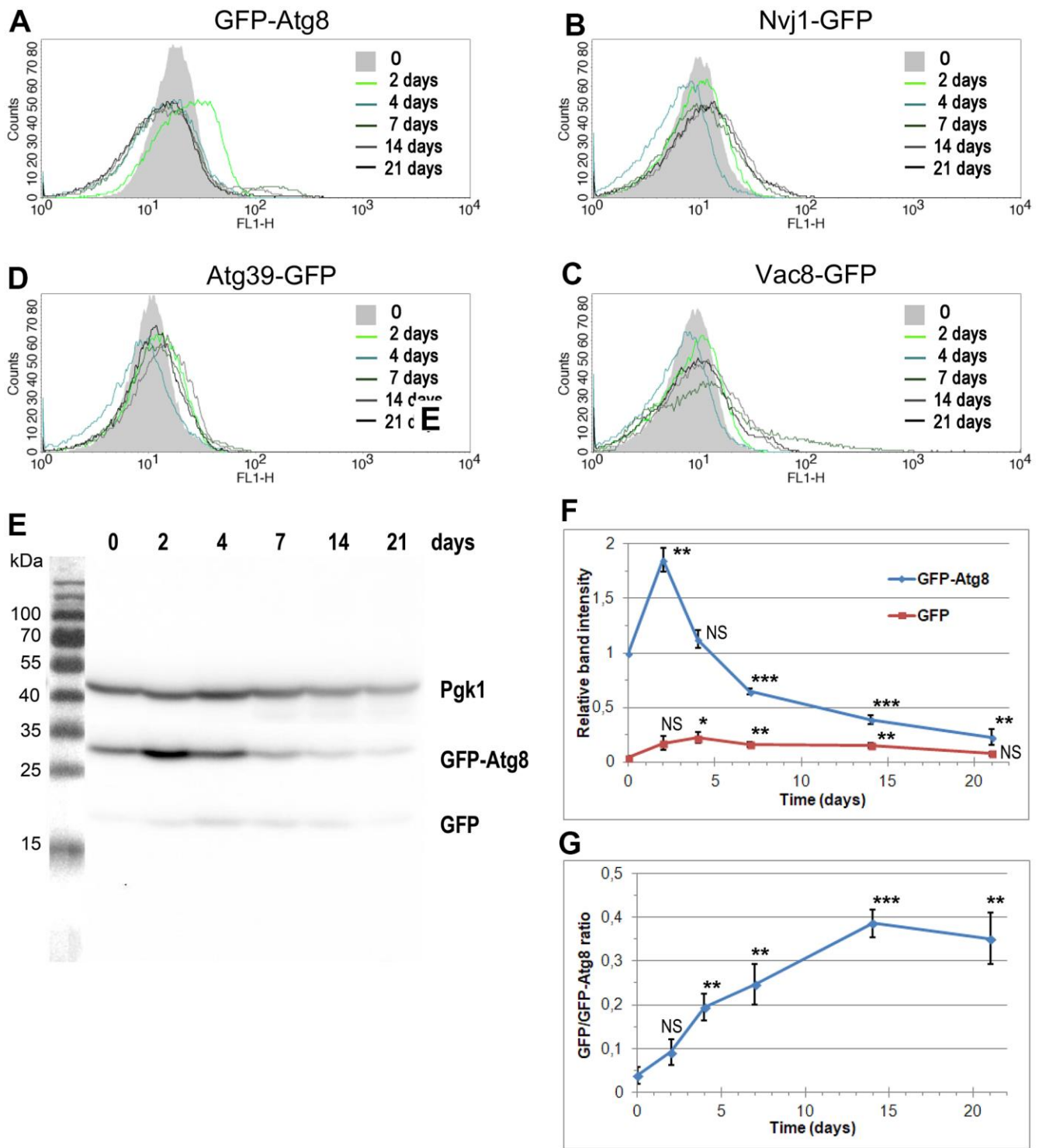


Figure 4. The changes in the level of autophagy markers during CLS assay. (A–D) The level of autophagy markers in the strains carrying fluorescently tagged GFP-Atg8 (YTE17) (A), Nvj1-GFP (YTE18) (B), Vac8-GFP (YTE19) (C), and Atg39-GFP (YTE20) (D) measured by flow cytometry. The mean from three independent biological repetitions is shown. (E) The level of GFP-Atg8 and its degradation product, free GFP, in the YTE17 strain, visualized by immunoblotting with anti-GFP antibody. One of three independent biological replicates is shown. (F, G) The quantification of western blot results. (F) The level of GFP-Atg8 and its degradation product GFP was normalized to the Pgk1 level and expressed relative to the GFP-Atg8 level at time 0 (protein level in the exponential growth phase). (G) The graph shows the GFP/GFP-Atg8 ratio at various time points. Data for each time point was normalized to the Pgk1 level. The mean of three biological replicates is shown for each time point. Bars indicate standard deviations. Statistical significance with respect to time 0 was assessed using the Student T-test (* $p < 0.05$; ** $p < 0.01$; *** $p < 0.001$; NS - non-significant).

the CLS experiment, the fluorescent signals fluctuated similarly. Cells expressing Nvj1-GFP, Vac8-GFP, and Atg39-GFP showed a slight increase in green fluorescence on the 2nd day, while on the 4th day, fluorescence decreased, to rise again on the 7th day. However, the scenarios were different for each of the analyzed proteins. In the case of Nvj1-GFP, fluorescence remained at the same level until the end of the CLS experiment. In the case of Atg39-GFP, fluorescence reached a maximum on the 14th day, decreasing later on. In the case of Vac8-GFP, we detected increasing fluorescence on the 7th and 14th day, with a decrease at the end of the CLS experiment. Additionally, the shape of the curve on the histogram changed, suggesting the presence of a subpopulation of cells with very high green fluorescence. These cells were most abundant on the 7th day of the CLS experiment.

The most significant change we observed while analyzing the fluorescence of GFP-Atg8 (Figure 4A). The histogram obtained for this protein shifted to the right on the 2nd day of the CLS experiment, indicating an increased Atg8 level at this time point in the whole cell population. On the 4th day, the level of Atg8 went back to an average level. However, on the 7th day of the CLS experiment, a subpopulation of cells with higher fluorescence appeared, persisting, albeit to a lesser extent, in the following days.

In parallel to the flow cytometry analysis, autophagy activity was measured with the GFP-Atg8 processing assay. Atg8 is efficiently degraded within the vacuole, but GFP is known to be resistant to proteolysis [47]. Subsequently, remains intact for longer, so it can be detected by Western blot and used to indicate nonselective autophagy [48]. Actually, we performed the biochemical assay to monitor both the changes in the Atg8 level and the release of free GFP from GFP-Atg8 in the population of aging cells in time. In Figure 4E–4G, the western blot analysis results are presented. Data showed a significant increase in the GFP-Atg8 level on the 2nd day of the CLS experiment (Figure 4F). We also noticed increasing with time GFP/GFP-Atg8 ratio, indicating the induction of autophagy in the analyzed cells (Figure 4G).

Nucleophagy and PMN are activated at different time points during chronological aging

Fluorescent tagging of proteins enables the tracking of changes in their cellular distribution. This technique has also been used to study autophagy induction. In the yeast species *S. cerevisiae*, autophagosome formation occurs at the phagophore assembly site (PAS), which is located adjacent to the vacuole [49]. Many of the Atg proteins assemble at the PAS to initiate phagophore

nucleation [50, 51]. Since most of the proteins involved in autophagy pathways are transiently associated with the PAS, it is possible to use fluorescence microscopy to assess their fluorescently tagged conjugates, which are localized in proximity to or already within a vacuole [40].

We used cells carrying selected fluorescently tagged autophagy markers (GFP-Atg8, Nvj1-GFP, Vac8-GFP, and Atg39-GFP) to track changes in their cellular levels and localization and to correlate their presence in the cell with the viability of tested cells. To indicate the vacuole location in the cell, we used the CellTracker Blue CMAC dye as a vacuole lumen marker. To distinguish between live and dead cells, we used PI staining. Fluorescence microscopy revealed changes in the localization of fluorescently tagged autophagy markers throughout the CLS experiment, suggesting the involvement of different autophagy pathways in aging. However, these pathways were used differently over time. We observed different kinetics of signal recruitment to vacuole contact sites and different times of signal internalization into the vacuole. Some signals also showed a temporary increase in intensity. The most visible increase in signal intensity was observed for GFP-Atg8 on the second day of the CLS experiment, which is consistent with flow cytometry and Western blot data (Figures 4A, 4E, 5A). As a marker of ongoing autophagy, GFP-Atg8 showed obvious phenotypes with sequential changes in signal patterns. First, an increase in the cellular level of the protein was observed, followed by its accumulation in the vicinity of the vacuole, with the PAS contact sites visible as very bright dots. Finally, the protein internalization was visible as an intense bright signal dispersed across the whole vacuole, which decreased with time. These sequential changes were detectable throughout the experiment, but their frequency changed over time (Figure 5A, 5C). The disappearance of the green signal was accompanied by an increase in the red signal of PI-stained cells, indicating cell death.

As shown in Figure 5 (see Supplementary Figure 2 for single-channel images), autophagy induction occurred in all analyzed strains (YTE18: *NVJ1-GFP*, YTE19: *VAC8-GFP*, and YTE20: *ATG39-GFP*), indicating that cells employ both nucleophagy and PMN during chronological aging. However, nucleophagy seems to be particularly engaged in the first few days. We observed Atg39-GFP internalization in a fraction of cells on the 2nd, 4th, and 7th day of the CLS experiment. In contrast, the PMN receptors appeared to be activated throughout the entire experiment. We concluded that nucleophagy is responsible for the initial drop in cell viability, while PMN contributes to cell survival until the end of the CLS experiment. These results are consistent with the findings of fluorescence microscopy studies.

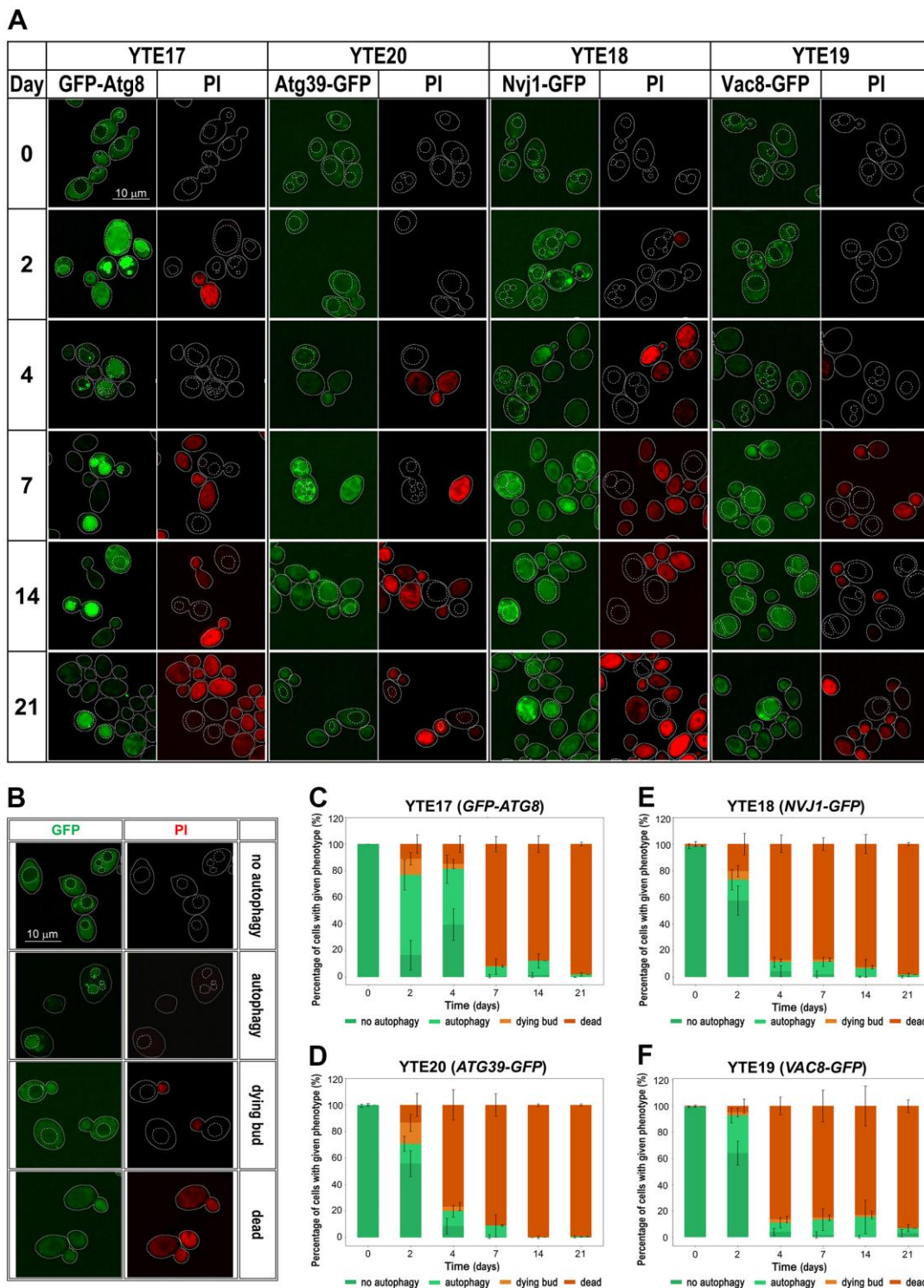


Figure 5. Changes in the autophagy markers' localization during chronological aging. (A) Microscopic analysis of strains carrying fluorescently tagged autophagy markers: YTE17 (*GFP-ATG8*), YTE20 (*ATG39-GFP*), YTE18 (*NVJ1-GFP*), and YTE19 (*VAC8-GFP*) in a given day of CLS experiment. Examples shown in (A) are focused on cells that were still viable at the analyzed time point. The microscopic images were collected and processed under the same conditions, so the differences in signal intensity are veritable. Cell borders are marked with solid lines, and vacuole outlines, determined based on CMAC staining, are marked with a dashed line. (B) Categories of counted phenotypes - examples. (C–F) The microscopic results quantification is shown as a percentage of cells presenting a given phenotype in the population from a specific time point. Three biological repetitions were performed; in each, at least 300 cells were analyzed for every time point. Graphs show the mean of all biological repetitions; whiskers represent standard deviations. Results obtained for YTE17 (*GFP-ATG8*) (C), YTE20 (*ATG39-GFP*) (D), YTE18 (*NVJ1-GFP*) (E), and YTE19 (*VAC8-GFP*) (F) are shown.

Furthermore, a detailed analysis of flow cytometry results provided additional findings on characterizing dying cells. We prepared histograms for individual subpopulations of living, dying, and dead cells defined as cells showing only green fluorescence (cells with GFP signal), showing high green and light red fluorescence (cells with an elevated level of GFP and limited ability to remove PI), and those with strong red fluorescence (cells stained by PI), respectively (Supplementary Figures 3–6). The histograms were prepared for each tested strain (YTE17: *GFP-ATG8*, YTE20: *ATG39-GFP*, YTE18: *NVJ1-GFP*, and YTE19: *VAC8-GFP*) at different time points during chronological aging (Figure 6). These histograms revealed that among cells with induced autophagy, those more prone to death were larger cells with buds. This was particularly evident on the 2nd and 4th days

of the CLS experiment in the YTE20 (*ATG39-GFP*) strain population, and from the 2nd day until at least the 7th day of the CLS experiment in the strains carrying fluorescently tagged PMN markers, YTE18 (*NVJ1-GFP*) and YTE19 (*VAC8-GFP*).

Interestingly, for the latter strains' populations, the histograms that reflect the cell size of living cell subpopulations changed to a bimodal distribution on the last two time points (14 and 21 days). In the histograms of YTE17 (*GFP-ATG8*) strains, the overrepresentation of budding cells among the dying cell population was visible only at the start of the CLS experiment (on the 2nd day). These data correlate with our former observations from fluorescence microscopy, where viable budding mother cells with dying buds were noticed (Figure 5A).

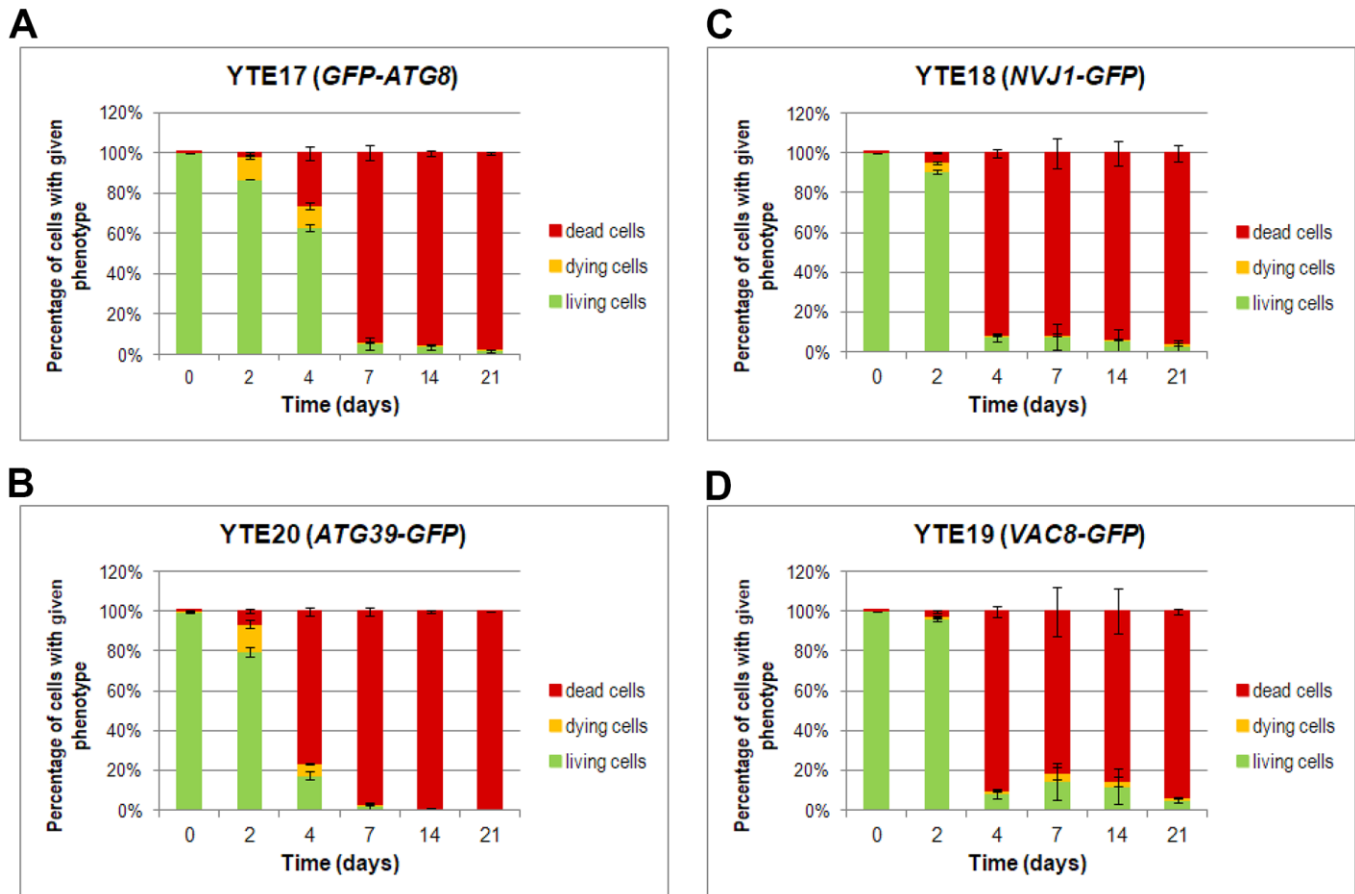


Figure 6. Changes in the cell viability during CLS, measured by flow cytometry. Cells of YTE17 (*GFP-ATG8*), YTE20 (*ATG39-GFP*), YTE18 (*NVJ1-GFP*), and YTE19 (*VAC8-GFP*) strains were stained with PI, and fluorescence signals were analyzed in two channels: FL1-H (for GFP) and FL2-H (for PI-stained cells) by flow cytometry in each day of the CLS experiment. According to the presented fluorescence signal, cells in the population were divided into three subpopulations: living, dying, and dead. See Supplementary Material Figures for gating conditions and histograms for each channel for strains and time points. (A–D) The flow cytometry results quantification was shown as a percentage of cells presenting a given phenotype in the population at a specific time point. Three biological repetitions were performed; and 10,000 events were analyzed for every strain and time point. Graphs show the mean of all biological repetitions; whiskers represent standard deviations. Results obtained for YTE17 (*GFP-ATG8*) (A), YTE20 (*ATG39-GFP*) (B), YTE18 (*NVJ1-GFP*) (C), and YTE19 (*VAC8-GFP*) (D) are shown.

DISCUSSION

The aging process affects many aspects of life, including at the cellular level, where it pertains to various molecules, such as DNA. As we age, there is an increase in cellular stress, which eventually affects DNA integrity [14, 15, 52]. In this study, we demonstrated that DNA undergoes extensive fragmentation during chronological aging. However, our earlier studies have shown that even highly fragmented DNA can be effectively rebuilt if the DNA repair pathways dedicated to its repair are available [53]. Nevertheless, all DNA damage, including the especially hazardous double-strand breaks (DSBs) that can compromise genome stability, must be repaired for cell survival. At this point, the non-homologous end joining (NHEJ) repair pathway is frequently involved, generating a highly rearranged chromosome where some sequences may even be lost. In such cases, the repaired genome becomes shorter, but the cell will survive as long as the lost fragments do not contain essential genes or sequences crucial for DNA maintenance processes.

Interestingly, a similar observation was reported recently for replicative aging. Mojumdar et al. [54] showed that during replicative aging, resection of DSBs (an early step of DSBs repair via homologous recombination) decreases, while at the same time, the usage of the other pathway of DSBs repair, NHEJ, increases. This results in an increased number of improper products of DSBs repair containing deletions and microhomologies. In chronologically aging cells, endogenously occurring DSBs seem to be defectively repaired, and the frequency of repair defects increases with time, likely leading to senescence [55].

In our studies on chronological aging, we observed a gradual depletion of DNA content in the population of analyzed diploid wild-type cells over time [36]. This result led us to question the mechanism of DNA disappearance and the minimum DNA content required for cell survival. We hypothesized that autophagy could be a probable cause of this phenomenon based on two reasons. First, at least two specialized autophagy pathways, namely nucleophagy and PMN, have been shown to be involved in the processing of nuclear content, including its DNA content [39, 56, 57]. Second, autophagy has been demonstrated to be involved in the chronological aging process [32].

Our data showed that nucleophagy and PMN are indeed activated during chronological aging but at different time points in the CLS experiment. The nucleophagy pathway was activated on the 2nd and 4th days of the CLS experiment, correlating with the steep decline in cell viability detected in the first days of the CLS assay. On the other hand, the PMN pathway was active

from the 4th day until the end of the CLS experiment. We concluded that nucleophagy leads to cell death, while PMN contributes to cell survival, likely by removing potentially recombinogenic DNA fragments from the nucleus, where they may provoke genome rearrangements. However, this piece-by-piece removal of genomic DNA may not last indefinitely, as there is a minimum DNA content required for life. According to our results, the minimal level of DNA allowing the survival of diploid cells is one copy of the genome, i.e., 1c DNA content.

Our CLS studies revealed an interesting observation that suggests that budding cells are more prone to death than mother cells. During the CLS experiment, we detected many cells whose buds were significantly stained with PI, while the mother cells were still vivid. We also observed cells with significantly higher GFP fluorescence in the bud than in the mother cells, as well as very small cells stained with PI but remarkably smaller than the average yeast cells. One of the possible explanations would be that budding cells, when trapped by starvation during chronological aging, might abandon mitosis and withdraw necessary compounds from the bud or even cut off the bud just to survive. However, proving such a hypothesis requires further investigation. This hypothesis contradicts the previously propagated belief concerning the relationship between mother and daughter cells, which claimed that mother cells would sacrifice themselves for the benefit of daughter cells, at least in the context of replicative aging rules [58–60]. However, this is not a general rule of life. For example, it has been shown that malnutrition, such as a lack of vitamin E, may lead to fetal resorption in pregnant animals, including humans. Thus, the hypothesis that follows the evolutionary idea of abandoning reproduction in limited nutritional resources is not so easily dismissed [61].

Recent research by Irvani et al. [62] suggests that yeast cells may indeed change their decision concerning starting a new replication round when nutrients are depleted after they have already passed the G1/S transition checkpoint (the START point of the cell cycle). The expression of G1/S transition genes depends on SBF (Swi4-Swi6) and MBF (Mbo1-Swi6) transcription activators and Whi5 repressor, and the nuclear localization of these transcription factors is regulated by phosphorylation. Dephosphorylated Whi5 can be re-imported into the nucleus, where it binds its target promoters until, upon replenishment of nutrients, CDK re-activation occurs, which releases transcription of G1/S transition genes [62].

What happens when tight control of the START point of the cell cycle is not possible? The answer is provided

by experiments in which Krol et al. describe the phenotypes of *swi6Δ* cells [63]. These cells lack functional G1/S transition genes transcription activator, and permanent replication stress leads to the formation of DSBs. The error-prone DNA repair pathway is then used, such as illegitimate recombination, leading to DNA content alterations, including aneuploidy, and resulting in high cell mortality [63]. Interestingly, under starvation conditions, budding yeast can be efficiently returned to the G1 phase in an autophagy-dependent manner. According to Matsui et al., autophagy prevents aberrant nuclear division that occurs despite insufficient cell growth, which can lead to an increased frequency of aneuploidy after supplementing a missing feed source [64]. Notably, we observed an overrepresentation of cells in the G1 phase on the 2nd and 4th day of the CLS assay (Figure 3E).

One more point should be taken into account when considering the mortality of chronologically aging cells: during starvation, yeast cells release autotoxins. It has been shown for many yeast species, including *Schizosaccharomyces pombe*, that cells release toxic compounds such as leucic acid and L-2-keto-3-methyl valerate during glucose depletion, which can kill sister cells [65]. A similar phenomenon of self-inhibition was noticed in *S. cerevisiae* aerobic fed-batch cultures [66]. The results showed that the growth decline observed in those cultures, even when maintained under optimal conditions, should be attributed to self-produced inhibitory compounds other than ethanol, likely cellular metabolites and toxic by-products [67]. These toxic compounds might be particularly harmful to cells with stress-induced transient membrane permeability [68]. It

is worth mentioning that the transition in membrane permeability is also observed during autophagy.

In recent years, much new data has emerged concerning the timing and protein-specificity dependence of various autophagy pathways, including nucleophagy and PMN, leading to some disorientation in the field. Receptor-like proteins such as Nvj1 and Vac8 were frequently used as suitable markers to follow PMN, and Atg39 was considered recommended for following nucleophagy [39, 56, 69]. However, recent *in vivo* data showed that the autophagy subpathways are not as specific and separable as previously thought. The same protein might contribute to both PMN and nucleophagy, as demonstrated in the context of Atg39 [67]. Additionally, the researchers' notion concerning the sequence of events that accompany the autophagy process appears not to be definitive. Mijaljica et al. previously showed that in nitrogen-starved, wild-type haploid yeast cells, PMN and so-called "late nucleophagy" are distinct in time, with PMN starting 3 h after acquiring starvation conditions, whereas nucleophagy can be detected only after prolonged periods of nitrogen starvation (after at least one day) [69]. However, our data suggested different scenarios, with nucleophagy starting first, followed by PMN.

Nevertheless, we must remember that the experimental conditions we used were different in many respects. We analyzed diploid cells for a much longer period, starting from the second day of starvation, under conditions typical of the CLS experiments. Our experimental model was tailored to the questions we asked, which focused on the fate of DNA during chronological aging.

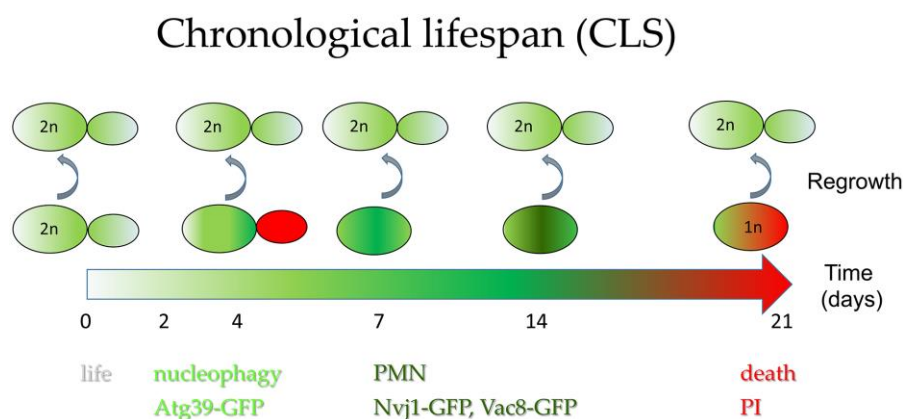


Figure 7. Autophagy contributes to cells' survival during chronological aging. Simplified hypothetical model of diploid cell aging showing (1) activation of nucleophagy at the time of the steepest drop in cells survival during CLS experiment and (2) activation of PMN allowing removal of damaged DNA from the nucleus, likely preventing DNA rearrangements. The unusual phenotype of temporal accumulation of cells with propidium iodide-labeled buds is encompassed in the scheme. This scheme also underlines that cellular DNA content is gradually lost with time during chronological aging, up to the haploid level. Still, only diploid cells can regrow. PMN - piecemeal microautophagy of nucleus; PI - propidium iodide-stained cells.

What would be the role of autophagy pathways during chronological aging in the context of cellular genome fate? We believe that the autophagy subpathways activated during chronological aging are crucial in (1) eliminating from the aging population cells that underwent aberrant mitosis; (2) preventing further entry into cell cycle phases, which prevents division abnormalities expected during starvation conditions; and (3) excluding from the nucleus potentially recombinogenic DNA fragments that may lead to DNA rearrangements.

One more issue should be addressed here, namely the puzzling result of the regrowth experiment. The way the regrowth experiment is performed excludes the possibility the regrown population is an offspring of diploids that survived the CLS experiment since the fraction of diploids at the end of the CLS experiment is too small to reach the observed density in the regrown cells population. We considered mating as a diploid source in the regrown population. However, mating is of low probability in a low-density culture containing a limited number of viable cells and intensively shaken. The alternative source of diploids would be endoreduplication. We currently believe it is the most probable source of diploids in the regrown population of aged cells, primarily since endoreduplication is known to occur in yeast [70].

CONCLUSIONS

We found that the chronological aging of diploid yeast *S. cerevisiae* cells is accompanied by extensive DNA fragmentation and a gradual loss of genomic DNA over time, which becomes lethal as soon as the DNA content of a given cell drops below $1c$. The highest decrease in cells' viability during chronological aging occurs when the nucleophagy pathway is activated, and the cell population is enriched in dying cells with PI-stained buds, with a prevalence of cells in the G1 phase. The further decrease in the chronological aging cells' DNA content seems dependent on PMN. We believe that this DNA depletion is linked to the clearance from the nucleus of potentially recombinogenic DNA fragments that could provoke DNA rearrangements. Thus, PMN contributes to genome maintenance and promotes survival in starvation conditions during aging (Figure 7). The fragmentation and loss of DNA is a known trait of dying cells also those subject to aging, especially in the context of cell death. The ability of aged cells with reduced ploidy to rebuild the diploid genome during regrowth was not, to our knowledge, documented before. The involvement of autophagy mechanisms in ploidy reduction suggests that it is not a random catastrophic event but a process beneficial to cell survival.

Since yeast cells are widely used as a eukaryotic cell model in aging research studies, we can extrapolate our results to higher eukaryotes. The chromosome fragmentation we documented during chronological aging and the subsequent engagement of autophagic pathways linked to the nucleus do resemble chromo-anagenesis in mammals. The observations we made in aging research using yeast as the eukaryotic cell model may help to understand the mechanisms that prevent aneuploidy during aging or cancerogenesis in cells where chromothripsis has occurred.

MATERIALS AND METHODS

Yeast strains

The diploid yeast strains used in this study were in the BY474X background and are listed in Table 1. They were the derivatives of the respective haploid strains taken from the library of *S. cerevisiae* strains carrying the genomic GFP-fusions of individual ORFs [71]. In these strains, the mating type was changed using transient expression of Ho endonuclease from the pGAL-HO.Ura plasmid [72]. The resulting *MAT α* strains were then crossed with the respective isogenic *MAT a* strains to obtain diploid homozygous in respect to the desired gene fusion encoding the selected autophagy marker proteins tagged with GFP. Obtained strains were tested by flow cytometry to confirm their ploidy.

Growth conditions and media

Yeast strains were grown in a minimal synthetic medium SCD containing 0.67% (w/v) Yeast nitrogen base without amino acids (Difco, Mt Pritchard, NSW, Australia), 2% (w/v) glucose (POCh, Gliwice, Poland) and amino acids (Formedium, Hunstanton, UK): L-leucine (180 mg/l), L-histidine (60 mg/l), uracil (60 mg/l) and methionine (60 mg/l). Each investigated strain was cultured in 120 ml of liquid medium, in 3 biological repeats. Cells were grown on a shaker at 150 rpm, 28° C for 21 days. At selected time points (0, i.e. exponential phase of growth, 2 days, 4 days, 7 days, 14 days and 21 days) 1×10^7 cells from each culture were harvested and subjected to further analyses.

In the regrowth experiment YPD medium, containing 1% yeast extract (Difco), 2% bactopectone (Difco), 2% glucose (POCh) was used. To obtain solid medium, 2% agar (Difco) was added.

Chronological lifespan (CLS) assays

Chronological lifespan of cells incubated in SCD medium was measured as previously described [36]. Briefly, from the growing culture, samples were removed

Table 1. Strains used in this study.

Strain	Genotype	Source
BY4741	<i>MATa his3Δ1 leu2Δ0 met15Δ0 ura3Δ0</i>	Euroscarf
BY4743	<i>MATa/Mata his3Δ1/his3Δ1 leu2Δ0/leu2Δ0 met15Δ0/met15Δ0 ura3Δ0/ura3Δ0</i>	Euroscarf
BY4741 GFP-ATG8	<i>MATa his3Δ1 leu2Δ0 met15Δ0 ura3Δ0 LYS2+ can1Δ::GAL1pr-Scel::STE2pr-SpHIS5 lyp1Δ::STE3pr-LEU2 ATG8p-sfGFP-ATG8</i>	SWAT [70]
BY4741 NVJ1-GFP	<i>MATa his3Δ1 leu2Δ0 met15Δ0 ura3Δ0 lys+ can1Δ::GAL1pr-Scel::STE2pr-SpHIS5; HPH::NVJ1p-NVJ1-sfGFP</i>	[70]
BY4741 ATG39-GFP	<i>MATa his3Δ1 leu2Δ0 met15Δ0 ura3Δ0 lys+ can1Δ::GAL1pr-Scel::STE2pr-SpHIS5; HPH::ATG39p-ATG39-sfGFP</i>	[70]
BY4741 VAC8-GFP	<i>MATa his3Δ1 leu2Δ0 met15Δ0 ura3Δ0 lys+ can1Δ::GAL1pr-Scel::STE2pr-SpHIS5; HPH::VAC8p-VAC8-sfGFP</i>	[70]
YAS433	<i>MATa his3Δ1 leu2Δ0 met15Δ0 ura3Δ0 lys+ can1Δ::GAL1pr-Scel::STE2pr-SpHIS5 lyp1Δ::STE3pr-LEU2 ATG8p-sfGFP-ATG8</i>	this work
YAS434	<i>MATa his3Δ1 leu2Δ0 met15Δ0 ura3Δ0 lys+ can1Δ::GAL1pr-Scel::STE2pr-SpHIS5; HPH::ATG39p-ATG39-sfGFP</i>	this work
YAS435	<i>MATa his3Δ1 leu2Δ0 met15Δ0 ura3Δ0 lys+ can1Δ::GAL1pr-Scel::STE2pr-SpHIS5; HPH::VAC8p-VAC8-sfGFP</i>	this work
YAS437	<i>MATa his3Δ1 leu2Δ0 met15Δ0 ura3Δ0 lys+ can1Δ::GAL1pr-Scel::STE2pr-SpHIS5; HPH::NVJ1p-NVJ1-sfGFP</i>	this work
YTE17	<i>MATa/Mata his3Δ1/his3Δ1 leu2Δ0/leu2Δ0 met15Δ0/met15Δ0 ura3Δ0/ura3Δ0 lys+can1Δ::GAL1pr-Scel::STE2pr-SpHIS5/can1Δ::GAL1pr-Scel::STE2pr-SpHIS5 lyp1Δ::STE3pr-LEU2/ lyp1Δ::STE3pr-LEU2 ATG8p-sfGFP-ATG8/ATG8p-sfGFP-ATG8</i>	this work
YTE18	<i>MATa/Mata his3Δ1/his3Δ1 leu2Δ0/leu2Δ0 met15Δ0/met15Δ0 ura3Δ0/ura3Δ0 lys+ can1Δ::GAL1pr-Scel::STE2pr-SpHIS5/can1Δ::GAL1pr-Scel::STE2pr-SpHIS5; HPH::NVJ1p-NVJ1-sfGFP/HPH::NVJ1p-NVJ1-sfGFP</i>	this work
YTE19	<i>MATa/Mata his3Δ1/his3Δ1 leu2Δ0/leu2Δ0 met15Δ0/met15Δ0 ura3Δ0/ura3Δ0 lys+ can1Δ::GAL1pr-Scel::STE2pr-SpHIS5/can1Δ::GAL1pr-Scel::STE2pr-SpHIS5; HPH::VAC8p-VAC8-sfGFP/HPH::VAC8p-VAC8-sfGFP</i>	this work
YTE20	<i>MATa/Mata his3Δ1/his3Δ1 leu2Δ0/leu2Δ0 met15Δ0/met15Δ0 ura3Δ0/ura3Δ0 lys+ can1Δ::GAL1pr-Scel::STE2pr-SpHIS5/can1Δ::GAL1pr-Scel::STE2pr-SpHIS5; HPH::ATG39p-ATG39-sfGFP/HPH::ATG39p-ATG39-sfGFP</i>	this work

at the indicated time points to assess the survival within the population. The number of colonies forming units (CFU) was counted for the samples taken after 2, 4, 7, 14, and 21 days of cultivation. The data from at least three independent experiments were averaged. Statistical significance of the results was assessed using ANOVA and Dunnett's post hoc test.

Regrowth assay

For the regrowth experiment, the 5 -10 μl of culture from a certain time-point of the CLS experiment was used to inoculate 20 ml of YPD medium. The 5 μl was used on the 2nd, 4th, and 7th days of CLS, while 10 μl for the 14th and 21st day. The cultures were cultivated with shaking at 28° C for 18 h until they reached the density of about 5 x 10⁶ cells per ml. Then, the cells were used for testing their phenotype, e.g., for DNA content analysis.

DNA content analysis by flow cytometry

The DNA content of yeast cells was measured by flow cytometry as previously described [21], with some modifications. Briefly, cells grown to exponential phase were fixed with 1 ml of chilled (-20° C) 80% ethanol, and then held at room temperature for at least 2 h. The fixed cells were washed twice using FACS buffer (0.2 M Tris-HCl (Sigma-Aldrich, St. Louis, MO, USA) pH 7.4 and 20 mM EDTA (Merck, Darmstadt, Germany)). To remove the RNA, cells suspensions were incubated in FACS buffer with 1 mg/ml RNase A (Sigma-Aldrich) for 2 h at 37° C. The cells were then washed with 1 x PBS, stained with 100 μl of PI solution (50 μg per ml) in 1 x PBS overnight at 4° C in the dark, and diluted with 900 μl of 1 x PBS. Prior to flow cytometry analysis, the cells were sonicated three times for 10 s in a Branson 2800 ultrasonic bath, to avoid cell clumping. The analysis of the DNA content was performed using a

FACSCalibur analyzer (Becton-Dickinson, Franklin Lakes, NJ, USA). A total of 10,000 cells in each sample were counted. At least three biological repetitions were assayed. Further data analysis was performed using CellQuestPro software (Becton-Dickinson).

The genome integrity analysis by electrophoretic methods

To assess yeast chromosome integrity in the aging cells, we separated yeast chromosomes by PFGE. The experiment was performed according to [63] with some modifications. Yeast cells of diploid BY4743 strain, from three biological repeats, were embedded in low-melting-point InCert agarose (Lonza, Basel, Switzerland), in 20 μ l plugs and digested with Zymolyase 100T (BioShop, Burlington, ON, Canada), then with proteinase K (Sigma-Aldrich) and RNase A at 30° C with gentle rotation (4 r.p.m.) on an SB3 rotator (Bibby Sterlin, Stone, UK). Plugs were placed in the wells of a gel prepared from 1.2% D5 agarose (Conda, Torrejon de Ardoz, Madrid, Spain) in 1 \times TAE and sealed with the same agarose. Electrophoresis was run in a CHEF Mapper® XA Pulsed-Field Electrophoresis System (Bio-Rad, Hercules, CA, USA) for 15 h in 1 \times TAE buffer at 6 V/cm and 12° C with the ramping set to 0.8, the angle set to 120°, and the switch time set to 65–90 s. After electrophoresis, the DNA was stained with SYBR™ Gold Nucleic Acid Gel Stain (Invitrogen, Carlsbad, CA, USA) for 30 min with gentle rocking, washed twice with water for 15 min, and documented by using 302-nm UV light for DNA visualization and a charge-coupled device camera (FluorChem Q Multi Image III, Alpha Innotech, San Leandro, CA, USA).

Agarose-embedded chromosomal DNA from the same cell samples was also separated in 1% D5 agarose gel using 15 h standard electrophoresis in 1 \times TAE buffer at 20 V/cm and 12° C. Gel was stained and documented as above.

Determination of GFP-Atg8 protein levels and GFP-Atg8 processing assay

The GFP-Atg8 and GFP levels change during CLS was assessed by western blot as in [73] with some modifications. Proteins were extracted from 1 \times 10⁸ cells collected at each time point during CLS using the TCA method, suspended in Laemmli sample buffer supplemented with 1 mM PMSF and cOmplete Protease Inhibitor Cocktail (Roche, Base, Switzerland), and boiled for 5 min. After centrifugation (19,300 g for 2 min), the equal volumes of the protein extracts were separated by SDS-PAGE (10% polyacrylamide gel), and the proteins were transferred onto PVDF membrane (GE Healthcare, Pittsburgh, PA, USA). Blots were blocked

for 2 h in 5% (w/v) nonfat dried milk + 5% (w/v) BSA (Sigma-Aldrich) in TBS-T [25mM Tris-HCl pH 7.5, 137 mM NaCl, 27 mM KCl, 0.1% (v/v) Tween-20]. GFP protein was detected with the rabbit polyclonal antibody anti-GFP (1:2000, Living Colors A.v. peptide antibody, 632377) and goat anti-rabbit IgG conjugated to horseradish peroxidase (HRP) (1:4000, Agilent, Cat# P0448, RRID:AB_2617138). Pgc1 was detected by using a mouse anti-Pgc1 antibody (1:10000, Abcam, Cat# ab113687, RRID:AB_10861977), followed by goat anti-mouse IgG conjugated to HRP (1:4000, Agilent, Cat# P0447, RRID:AB_2617137). Immunoreactive proteins on the blots were visualized using chemiluminescent substrates: SuperSignal WestFemto, (Thermo Fisher Scientific Inc., Waltham, MA, USA) and documented with a charge-coupled device camera (FluorChem Q Multi Image III, Alpha Innotech, San Leandro, CA, USA). The resulting bands were quantified by using Image Quant 5.2 (Molecular Dynamics, Inc., Sunnyvale, CA, USA). The GFP-Atg8 and GFP protein levels were normalized to those of Pgc1. The mean of three biological repetitions were averaged to determine the relative protein levels for each time point of CLS. The GFP/GFP-Atg8 ratio was also calculated. Statistical significance with respect to time 0 was assessed using the Student T-test.

Autophagy induction studies using fluorescence microscopy

Strains carrying the fluorescently tagged autophagy markers (GFP-Atg8, Atg39-GFP, Nvj1-GFP, and Vac8-GFP) were used together with two fluorescent dyes staining the vacuole (CellTracker™ Blue CMAC Dye, Invitrogen) and dead cells (PI, Calbiochem, San Diego, CA, USA) respectively. We followed the changes in the cellular localization of autophagy markers and the correlation between their presence in the cell and the viability of tested cells. Autophagy induction occurs when autophagy markers co-localize with the vacuole.

Harvested cells of strains assigned for fluorescence microscopy analysis were first stained with PI (final concentration 0.1 mg/ml) and CellTracker™ Blue CMAC Dye (final concentration 50 μ M) for 30 minutes at room temperature in the dark. Stained cells were washed three times with 1 \times PBS. After washing, pelleted cells were suspended in 30 μ l of 1 \times PBS. The 3 μ l of analyzed cells' suspension was placed on a microscope slide for microscopic analysis. Imaging was performed using Zeiss AxioCam MRc5 Digital Camera (Zeiss, Oberkochen, Germany), mounted on Zeiss Axio Imager.M2 fluorescence microscope operated by Zeiss Axio Vision 4.8 software using: DIC (for bright field), and 49HE, 63HE, and 38HE filter sets (for CMAC, PI, and GFP, respectively). All

images were acquired with 100-fold magnification under immersion oil. Fluorescent microscopy images quantitative analysis was performed using Fiji software, using Cell Counter and DeconvolutionLab2 plugins.

Flow cytometry measurement of autophagy markers level and cells' viability during CLS

Strains carrying the fluorescently tagged autophagy markers (GFP-Atg8, Atg39-GFP, Nvj1-GFP, and Vac8-GFP) were analyzed by flow cytometry during the CLS experiment. Half of the culture of the tested strain from the given time point of CLS was stained with 0.1 mg/ml PI (Calbiochem, San Diego, CA, USA) in 1 x PBS for 30 minutes in the dark to assess the cells' viability. PI stains only dead cells. By analyzing both unstained and stained cells, we followed two parameters: (1) the changes in the autophagy markers' levels, which are believed to increase during autophagy induction; and (2) the correlation between increased autophagy marker signal and viability of tested cells.

The analysis was performed using a FACSCalibur analyzer (Becton-Dickinson, Franklin Lakes, NJ, USA). A total of 10,000 cells in each sample were counted. At least three biological repetitions were assayed. Farther data analysis was performed using CellQuestPro software (Becton-Dickinson).

Availability of data and materials

All data generated or analyzed during this study are included in this published article and its Supplementary Information Files.

Abbreviations

CFU: colony forming units; CLS: chronological lifespan; DSB: double-strand break; NHEJ: non-homologous end joining; PFGE: pulse-field gel electrophoresis; PI: propidium iodide; PMN: piecemeal microautophagy of nucleus; RLS: replicative lifespan.

AUTHOR CONTRIBUTIONS

Conception of the study AS, TE and MS. All authors contributed to the study design. KS and MM performed CLS assay. TE and AS constructed the strains. TE performed MF studies. MS performed WB analysis. AS performed flow cytometry analysis. All authors contributed to statistical data analysis. The first draft of the manuscript was written by AS, all authors commented on previous versions of the manuscript. All authors read and approved the final manuscript.

ACKNOWLEDGMENTS

We thank Maya Schuldiner for the strains.

CONFLICTS OF INTEREST

The authors declare that they have no conflicts of interest.

FUNDING

This work was supported by the National Science Center grant 2016/21/B/NZ3/03641.

REFERENCES

1. Bilinski T, Bylak A, Zadrag-Tecza R. The budding yeast *Saccharomyces cerevisiae* as a model organism: possible implications for gerontological studies. *Biogerontology*. 2017; 18:631–40. <https://doi.org/10.1007/s10522-017-9712-x> PMID:[28573416](https://pubmed.ncbi.nlm.nih.gov/28573416/)
2. He C, Zhou C, Kennedy BK. The yeast replicative aging model. *Biochim Biophys Acta Mol Basis Dis*. 2018; 1864:2690–6. <https://doi.org/10.1016/j.bbadis.2018.02.023> PMID:[29524633](https://pubmed.ncbi.nlm.nih.gov/29524633/)
3. Legon L, Rallis C. Genome-wide screens in yeast models towards understanding chronological lifespan regulation. *Brief Funct Genomics*. 2022; 21:4–12. <https://doi.org/10.1093/bfpg/elab011> PMID:[33728458](https://pubmed.ncbi.nlm.nih.gov/33728458/)
4. Molon M, Zadrag-Tecza R, Bilinski T. The longevity in the yeast *Saccharomyces cerevisiae*: A comparison of two approaches for assessment the lifespan. *Biochem Biophys Res Commun*. 2015; 460:651–6. <https://doi.org/10.1016/j.bbrc.2015.03.085> PMID:[25817783](https://pubmed.ncbi.nlm.nih.gov/25817783/)
5. Minois N, Frajnt M, Wilson C, Vaupel JW. Advances in measuring lifespan in the yeast *Saccharomyces cerevisiae*. *Proc Natl Acad Sci USA*. 2005; 102:402–6. <https://doi.org/10.1073/pnas.0408332102> PMID:[15625107](https://pubmed.ncbi.nlm.nih.gov/15625107/)
6. Mortimer RK, Johnston JR. Life span of individual yeast cells. *Nature*. 1959; 183:1751–2. <https://doi.org/10.1038/1831751a0> PMID:[13666896](https://pubmed.ncbi.nlm.nih.gov/13666896/)
7. Longo VD, Fabrizio P. Chronological aging in *Saccharomyces cerevisiae*. *Subcell Biochem*. 2012; 57:101–21. https://doi.org/10.1007/978-94-007-2561-4_5 PMID:[22094419](https://pubmed.ncbi.nlm.nih.gov/22094419/)
8. Lavoie H, Whiteway M. Increased respiration in the sch9Delta mutant is required for increasing

- chronological life span but not replicative life span. *Eukaryot Cell*. 2008; 7:1127–35.
<https://doi.org/10.1128/EC.00330-07>
PMID:18469137
9. Hlavatá L, Nachin L, Jezek P, Nyström T. Elevated Ras/protein kinase A activity in *Saccharomyces cerevisiae* reduces proliferation rate and lifespan by two different reactive oxygen species-dependent routes. *Aging Cell*. 2008; 7:148–57.
<https://doi.org/10.1111/j.1474-9726.2007.00361.x>
PMID:18081742
 10. Wakatsuki T, Sasaki M, Kobayashi T. Defects in the NuA4 acetyltransferase complex increase stability of the ribosomal RNA gene and extend replicative lifespan. *Genes Genet Syst*. 2019; 94:197–206.
<https://doi.org/10.1266/ggs.19-00022> PMID:31694990
 11. Kaeberlein M, McVey M, Guarente L. The SIR2/3/4 complex and SIR2 alone promote longevity in *Saccharomyces cerevisiae* by two different mechanisms. *Genes Dev*. 1999; 13:2570–80.
<https://doi.org/10.1101/gad.13.19.2570>
PMID:10521401
 12. Smith JT, White JW, Dungrawala H, Hua H, Schneider BL. Yeast lifespan variation correlates with cell growth and SIR2 expression. *PLoS One*. 2018; 13:e0200275.
<https://doi.org/10.1371/journal.pone.0200275>
PMID:29979754
 13. Steffen KK, MacKay VL, Kerr EO, Tsuchiya M, Hu D, Fox LA, Dang N, Johnston ED, Oakes JA, Tchao BN, Pak DN, Fields S, Kennedy BK, Kaeberlein M. Yeast life span extension by depletion of 60s ribosomal subunits is mediated by Gcn4. *Cell*. 2008; 133:292–302.
<https://doi.org/10.1016/j.cell.2008.02.037>
PMID:18423200
 14. Crane MM, Russell AE, Schafer BJ, Blue BW, Whalen R, Almazan J, Hong MG, Nguyen B, Goings JE, Chen KL, Kelly R, Kaeberlein M. DNA damage checkpoint activation impairs chromatin homeostasis and promotes mitotic catastrophe during aging. *Elife*. 2019; 8:e50778.
<https://doi.org/10.7554/eLife.50778>
PMID:31714209
 15. Tomblin G, Millen JI, Plevoda B, Rapaport M, Baxter B, Van Meter M, Gilbertson M, Madrey J, Piazza GA, Rasmussen L, Wennerberg K, White EL, Nitiss JL, Goldfarb DS. Effects of an unusual poison identify a lifespan role for Topoisomerase 2 in *Saccharomyces cerevisiae*. *Aging (Albany NY)*. 2017; 9:68–97.
<https://doi.org/10.18632/aging.101114>
PMID:28077781
 16. Hotz M, Thayer NH, Hendrickson DG, Schinski EL, Xu J, Gottschling DE. rDNA array length is a major determinant of replicative lifespan in budding yeast. *Proc Natl Acad Sci USA*. 2022; 119:e2119593119.
<https://doi.org/10.1073/pnas.2119593119>
PMID:35394872
 17. Higuchi-Sanabria R, Vevea JD, Charalel JK, Sapor ML, Pon LA. The transcriptional repressor Sum1p counteracts Sir2p in regulation of the actin cytoskeleton, mitochondrial quality control and replicative lifespan in *Saccharomyces cerevisiae*. *Microb Cell*. 2016; 3:79–88.
<https://doi.org/10.15698/mic2016.02.478>
PMID:28357337
 18. Garcia EJ, de Jonge JJ, Liao PC, Stivison E, Sing CN, Higuchi-Sanabria R, Boldogh IR, Pon LA. Reciprocal interactions between mtDNA and lifespan control in budding yeast. *Mol Biol Cell*. 2019; 30:2943–52.
<https://doi.org/10.1091/mbc.E18-06-0356>
PMID:31599702
 19. Molon M, Szajwaj M, Tchorzewski M, Skoczowski A, Niewiadomska E, Zdrag-Tecza R. The rate of metabolism as a factor determining longevity of the *Saccharomyces cerevisiae* yeast. *Age (Dordr)*. 2016; 38:11.
<https://doi.org/10.1007/s11357-015-9868-8>
PMID:26783001
 20. Gourlay CW, Carpp LN, Timpson P, Winder SJ, Ayscough KR. A role for the actin cytoskeleton in cell death and aging in yeast. *J Cell Biol*. 2004; 164:803–9.
<https://doi.org/10.1083/jcb.200310148>
PMID:15024029
 21. Zdrag-Tecza R, Kwolek-Mirek M, Alabrudzińska M, Skoneczna A. Cell Size Influences the Reproductive Potential and Total Lifespan of the *Saccharomyces cerevisiae* Yeast as Revealed by the Analysis of Polyploid Strains. *Oxid Med Cell Longev*. 2018; 2018:1898421.
<https://doi.org/10.1155/2018/1898421>
PMID:29743970
 22. Molon M, Woznicka O, Zebrowski J. Cell wall biosynthesis impairment affects the budding lifespan of the *Saccharomyces cerevisiae* yeast. *Biogerontology*. 2018; 19:67–79.
<https://doi.org/10.1007/s10522-017-9740-6>
PMID:29189912
 23. Bari KA, Berg MD, Genereaux J, Brandl CJ, Lajoie P. Tra1 controls the transcriptional landscape of the aging cell. *G3 (Bethesda)*. 2023; 13:jkac287.
<https://doi.org/10.1093/g3journal/jkac287>
PMID:36315064
 24. Kane AE, Sinclair DA. Epigenetic changes during aging and their reprogramming potential. *Crit Rev Biochem Mol Biol*. 2019; 54:61–83.

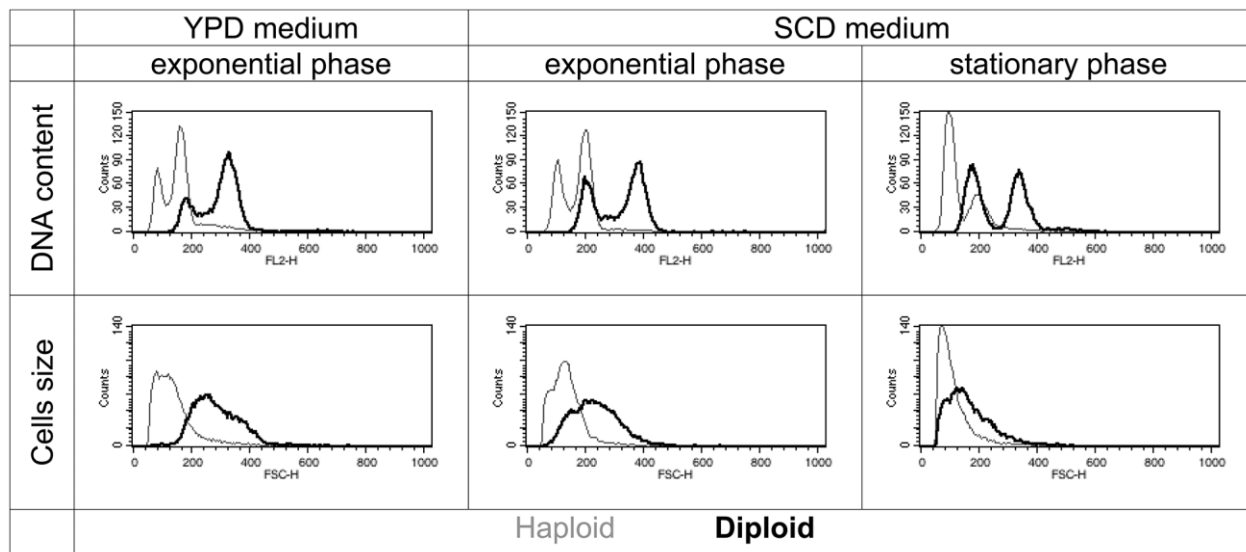
- <https://doi.org/10.1080/10409238.2019.1570075>
PMID:[30822165](https://pubmed.ncbi.nlm.nih.gov/30822165/)
25. Chadwick SR, Fazio EN, Etedali-Zadeh P, Genereaux J, Duennwald ML, Lajoie P. A functional unfolded protein response is required for chronological aging in *Saccharomyces cerevisiae*. *Curr Genet*. 2020; 66:263–77.
<https://doi.org/10.1007/s00294-019-01019-0>
PMID:[31346745](https://pubmed.ncbi.nlm.nih.gov/31346745/)
26. Medkour Y, Titorenko VI. Mitochondria operate as signaling platforms in yeast aging. *Aging (Albany NY)*. 2016; 8:212–3.
<https://doi.org/10.18632/aging.100914>
PMID:[26928478](https://pubmed.ncbi.nlm.nih.gov/26928478/)
27. Deb R, Nagotu S. The nexus between peroxisome abundance and chronological ageing in *Saccharomyces cerevisiae*. *Biogerontology*. 2023; 24:81–97.
<https://doi.org/10.1007/s10522-022-09992-9>
PMID:[36209442](https://pubmed.ncbi.nlm.nih.gov/36209442/)
28. Zahoor H, Watchaputi K, Hata J, Pabuprapap W, Suksamrarn A, Chua LS, Soontorngun N. Model yeast as a versatile tool to examine the antioxidant and anti-ageing potential of flavonoids, extracted from medicinal plants. *Front Pharmacol*. 2022; 13:980066.
<https://doi.org/10.3389/fphar.2022.980066>
PMID:[36120300](https://pubmed.ncbi.nlm.nih.gov/36120300/)
29. Mołoń M, Molestak E, Kula-Maximenko M, Grela P, Tchórzewski M. Ribosomal Protein uL11 as a Regulator of Metabolic Circuits Related to Aging and Cell Cycle. *Cells*. 2020; 9:1745.
<https://doi.org/10.3390/cells9071745> PMID:[32708309](https://pubmed.ncbi.nlm.nih.gov/32708309/)
30. Cao L, Tang Y, Quan Z, Zhang Z, Oliver SG, Zhang N. Chronological Lifespan in Yeast Is Dependent on the Accumulation of Storage Carbohydrates Mediated by Yak1, Mck1 and Rim15 Kinases. *PLoS Genet*. 2016; 12:e1006458.
<https://doi.org/10.1371/journal.pgen.1006458>
PMID:[27923067](https://pubmed.ncbi.nlm.nih.gov/27923067/)
31. Yu S, Zhang XE, Chen G, Liu W. Compromised cellular responses to DNA damage accelerate chronological aging by incurring cell wall fragility in *Saccharomyces cerevisiae*. *Mol Biol Rep*. 2012; 39:3573–83.
<https://doi.org/10.1007/s11033-011-1131-5>
PMID:[21713403](https://pubmed.ncbi.nlm.nih.gov/21713403/)
32. Smith DL Jr, Maharrey CH, Carey CR, White RA, Hartman JL 4th. Gene-nutrient interaction markedly influences yeast chronological lifespan. *Exp Gerontol*. 2016; 86:113–23.
<https://doi.org/10.1016/j.exger.2016.04.012>
PMID:[27125759](https://pubmed.ncbi.nlm.nih.gov/27125759/)
33. Delaney JR, Murakami C, Chou A, Carr D, Schleit J, Sutphin GL, An EH, Castanza AS, Fletcher M, Goswami S, Higgins S, Holmberg M, Hui J, et al. Dietary restriction and mitochondrial function link replicative and chronological aging in *Saccharomyces cerevisiae*. *Exp Gerontol*. 2013; 48:1006–13.
<https://doi.org/10.1016/j.exger.2012.12.001>
PMID:[23235143](https://pubmed.ncbi.nlm.nih.gov/23235143/)
34. Zou K, Rouskin S, Dervishi K, McCormick MA, Sasikumar A, Deng C, Chen Z, Kaeberlein M, Brem RB, Polymenis M, Kennedy BK, Weissman JS, Zheng J, et al. Life span extension by glucose restriction is abrogated by methionine supplementation: Cross-talk between glucose and methionine and implication of methionine as a key regulator of life span. *Sci Adv*. 2020; 6:eaba1306.
<https://doi.org/10.1126/sciadv.aba1306>
PMID:[32821821](https://pubmed.ncbi.nlm.nih.gov/32821821/)
35. Liu Y, Liu N, Wu D, Bi Q, Meng S. The longevity of tor1Δ, sch9Δ, and ras2Δ mutants depends on actin dynamics in *Saccharomyces cerevisiae*. *Cell Biosci*. 2015; 5:18.
<https://doi.org/10.1186/s13578-015-0008-z>
PMID:[25901273](https://pubmed.ncbi.nlm.nih.gov/25901273/)
36. Stępień K, Skoneczna A, Kula-Maximenko M, Jurczyk Ł, Mołoń M. Depletion of the Origin Recognition Complex Subunits Delays Aging in Budding Yeast. *Cells*. 2022; 11:1252.
<https://doi.org/10.3390/cells11081252>
PMID:[35455932](https://pubmed.ncbi.nlm.nih.gov/35455932/)
37. Mirisola MG, Longo VD. Yeast Chronological Lifespan: Longevity Regulatory Genes and Mechanisms. *Cells*. 2022; 11:1714.
<https://doi.org/10.3390/cells11101714>
PMID:[35626750](https://pubmed.ncbi.nlm.nih.gov/35626750/)
38. Moreno DF, Jenkins K, Morlot S, Charvin G, Csikasz-Nagy A, Aldea M. Proteostasis collapse, a hallmark of aging, hinders the chaperone-Start network and arrests cells in G1. *Elife*. 2019; 8:e48240.
<https://doi.org/10.7554/eLife.48240>
PMID:[31518229](https://pubmed.ncbi.nlm.nih.gov/31518229/)
39. Papandreou ME, Tavernarakis N. Nucleophagy: from homeostasis to disease. *Cell Death Differ*. 2019; 26:630–9.
<https://doi.org/10.1038/s41418-018-0266-5>
PMID:[30647432](https://pubmed.ncbi.nlm.nih.gov/30647432/)
40. Delorme-Axford E, Guimaraes RS, Reggiori F, Klionsky DJ. The yeast *Saccharomyces cerevisiae*: an overview of methods to study autophagy progression. *Methods*. 2015; 75:3–12.
<https://doi.org/10.1016/j.ymeth.2014.12.008>
PMID:[25526918](https://pubmed.ncbi.nlm.nih.gov/25526918/)
41. Kirisako T, Baba M, Ishihara N, Miyazawa K, Ohsumi M, Yoshimori T, Noda T, Ohsumi Y. Formation process of

- autophagosome is traced with Apg8/Aut7p in yeast. *J Cell Biol.* 1999; 147:435–46.
<https://doi.org/10.1083/jcb.147.2.435> PMID:[10525546](https://pubmed.ncbi.nlm.nih.gov/10525546/)
42. Huang WP, Scott SV, Kim J, Klionsky DJ. The itinerary of a vesicle component, Aut7p/Cvt5p, terminates in the yeast vacuole via the autophagy/Cvt pathways. *J Biol Chem.* 2000; 275:5845–51.
<https://doi.org/10.1074/jbc.275.8.5845>
 PMID:[10681575](https://pubmed.ncbi.nlm.nih.gov/10681575/)
 43. Shu WJ, Zhao MJ, Klionsky DJ, Du HN. Old factors, new players: transcriptional regulation of autophagy. *Autophagy.* 2020; 16:956–8.
<https://doi.org/10.1080/15548627.2020.1728611>
 PMID:[32054419](https://pubmed.ncbi.nlm.nih.gov/32054419/)
 44. Worley J, Luo X, Capaldi AP. Inositol pyrophosphates regulate cell growth and the environmental stress response by activating the HDAC Rpd3L. *Cell Rep.* 2013; 3:1476–82.
<https://doi.org/10.1016/j.celrep.2013.03.043>
 PMID:[23643537](https://pubmed.ncbi.nlm.nih.gov/23643537/)
 45. Nagarajan S, Kruckeberg AL, Schmidt KH, Kroll E, Hamilton M, McInerney K, Summers R, Taylor T, Rosenzweig F. Uncoupling reproduction from metabolism extends chronological lifespan in yeast. *Proc Natl Acad Sci USA.* 2014; 111:E1538–47.
<https://doi.org/10.1073/pnas.1323918111>
 PMID:[24706810](https://pubmed.ncbi.nlm.nih.gov/24706810/)
 46. Chasman D, Ho YH, Berry DB, Nemecek CM, MacGilvray ME, Hose J, Merrill AE, Lee MV, Will JL, Coon JJ, Ansari AZ, Craven M, Gasch AP. Pathway connectivity and signaling coordination in the yeast stress-activated signaling network. *Mol Syst Biol.* 2014; 10:759.
<https://doi.org/10.15252/msb.20145120>
 PMID:[25411400](https://pubmed.ncbi.nlm.nih.gov/25411400/)
 47. Bokman SH, Ward WW. Renaturation of Aequorea gree-fluorescent protein. *Biochem Biophys Res Commun.* 1981; 101:1372–80.
[https://doi.org/10.1016/0006-291x\(81\)91599-0](https://doi.org/10.1016/0006-291x(81)91599-0)
 PMID:[7306136](https://pubmed.ncbi.nlm.nih.gov/7306136/)
 48. Welter E, Thumm M, Krick R. Quantification of nonselective bulk autophagy in *S. cerevisiae* using Pgl1-GFP. *Autophagy.* 2010; 6:794–7.
<https://doi.org/10.4161/auto.6.6.12348>
 PMID:[20523132](https://pubmed.ncbi.nlm.nih.gov/20523132/)
 49. Gatica D, Wen X, Cheong H, Klionsky DJ. Vac8 determines phagophore assembly site vacuolar localization during nitrogen starvation-induced autophagy. *Autophagy.* 2021; 17:1636–48.
<https://doi.org/10.1080/15548627.2020.1776474>
 PMID:[32508216](https://pubmed.ncbi.nlm.nih.gov/32508216/)
 50. Xie Z, Klionsky DJ. Autophagosome formation: core machinery and adaptations. *Nat Cell Biol.* 2007; 9:1102–9.
<https://doi.org/10.1038/ncb1007-1102>
 PMID:[17909521](https://pubmed.ncbi.nlm.nih.gov/17909521/)
 51. He C, Klionsky DJ. Regulation mechanisms and signaling pathways of autophagy. *Annu Rev Genet.* 2009; 43:67–93.
<https://doi.org/10.1146/annurev-genet-102808-114910> PMID:[19653858](https://pubmed.ncbi.nlm.nih.gov/19653858/)
 52. Thongsroy J, Patchsung M, Pongpanich M, Settayanon S, Mutirangura A. Reduction in replication-independent endogenous DNA double-strand breaks promotes genomic instability during chronological aging in yeast. *FASEB J.* 2018. [Epub ahead of print].
<https://doi.org/10.1096/fj.201800218RR>
 PMID:[29812972](https://pubmed.ncbi.nlm.nih.gov/29812972/)
 53. Krol K, Brozda I, Skoneczny M, Bretner M, Skoneczna A. A genomic screen revealing the importance of vesicular trafficking pathways in genome maintenance and protection against genotoxic stress in diploid *Saccharomyces cerevisiae* cells. *PLoS One.* 2015; 10:e0120702.
<https://doi.org/10.1371/journal.pone.0120702>
 PMID:[25756177](https://pubmed.ncbi.nlm.nih.gov/25756177/)
 54. Mojumdar A, Mair N, Adam N, Cobb JA. Changes in DNA double-strand break repair during aging correlate with an increase in genomic mutations. *J Mol Biol.* 2022; 434:167798.
<https://doi.org/10.1016/j.jmb.2022.167798>
 PMID:[35998703](https://pubmed.ncbi.nlm.nih.gov/35998703/)
 55. Pongpanich M, Patchsung M, Mutirangura A. Pathologic Replication-Independent Endogenous DNA Double-Strand Breaks Repair Defect in Chronological Aging Yeast. *Front Genet.* 2018; 9:501.
<https://doi.org/10.3389/fgene.2018.00501>
 PMID:[30410502](https://pubmed.ncbi.nlm.nih.gov/30410502/)
 56. Mochida K, Oikawa Y, Kimura Y, Kirisako H, Hirano H, Ohsumi Y, Nakatogawa H. Receptor-mediated selective autophagy degrades the endoplasmic reticulum and the nucleus. *Nature.* 2015; 522:359–62.
<https://doi.org/10.1038/nature14506> PMID:[26040717](https://pubmed.ncbi.nlm.nih.gov/26040717/)
 57. Otto FB, Thumm M. Mechanistic dissection of macro- and micronucleophagy. *Autophagy.* 2021; 17:626–39.
<https://doi.org/10.1080/15548627.2020.1725402>
 PMID:[32046569](https://pubmed.ncbi.nlm.nih.gov/32046569/)
 58. Henderson KA, Gottschling DE. A mother's sacrifice: what is she keeping for herself? *Curr Opin Cell Biol.* 2008; 20:723–8.
<https://doi.org/10.1016/j.ceb.2008.09.004>
 PMID:[18848886](https://pubmed.ncbi.nlm.nih.gov/18848886/)
 59. Kennedy BK, McCormick MA. Asymmetric segregation: the shape of things to come? *Curr Biol.* 2011; 21:R149–51.

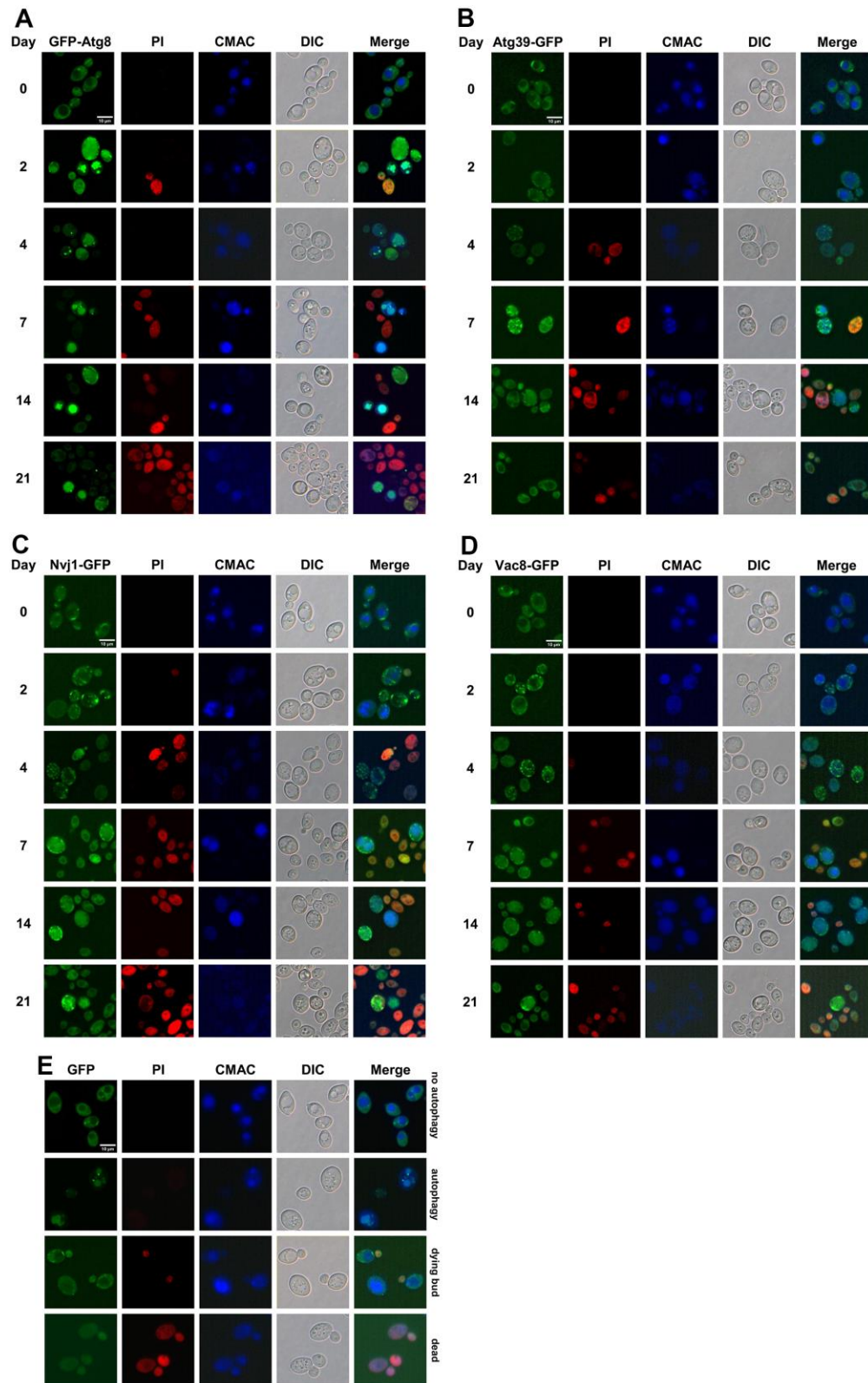
- <https://doi.org/10.1016/j.cub.2011.01.018>
PMID:[21334292](https://pubmed.ncbi.nlm.nih.gov/21334292/)
60. Yang J, McCormick MA, Zheng J, Xie Z, Tsuchiya M, Tsuchiyama S, El-Samad H, Ouyang Q, Kaeberlein M, Kennedy BK, Li H. Systematic analysis of asymmetric partitioning of yeast proteome between mother and daughter cells reveals “aging factors” and mechanism of lifespan asymmetry. *Proc Natl Acad Sci USA*. 2015; 112:11977–82.
<https://doi.org/10.1073/pnas.1506054112>
PMID:[26351681](https://pubmed.ncbi.nlm.nih.gov/26351681/)
61. Niki E, Traber MG. A history of vitamin E. *Ann Nutr Metab*. 2012; 61:207–12.
<https://doi.org/10.1159/000343106>
PMID:[23183290](https://pubmed.ncbi.nlm.nih.gov/23183290/)
62. Irvani D, Schlottmann FP, Muralidhara P, Nadelson I, Kleemann K, Wood NE, Doncic A, Ewald JC. When yeast cells change their mind: cell cycle “Start” is reversible under starvation. *EMBO J*. 2023; 42:e110321.
<https://doi.org/10.15252/emboj.2021110321>
PMID:[36420556](https://pubmed.ncbi.nlm.nih.gov/36420556/)
63. Krol K, Antoniuk-Majchrzak J, Skoneczny M, Sienko M, Jendrysek J, Rumieniczuk I, Halas A, Kurlandzka A, Skoneczna A. Lack of G1/S control destabilizes the yeast genome via replication stress-induced DSBs and illegitimate recombination. *J Cell Sci*. 2018; 131:jcs226480.
<https://doi.org/10.1242/jcs.226480> PMID:[30463853](https://pubmed.ncbi.nlm.nih.gov/30463853/)
64. Matsui A, Kamada Y, Matsuura A. The role of autophagy in genome stability through suppression of abnormal mitosis under starvation. *PLoS Genet*. 2013; 9:e1003245.
<https://doi.org/10.1371/journal.pgen.1003245>
PMID:[23382696](https://pubmed.ncbi.nlm.nih.gov/23382696/)
65. Oda AH, Tamura M, Kaneko K, Ohta K, Hatakeyama TS. Autotoxin-mediated latecomer killing in yeast communities. *PLoS Biol*. 2022; 20:e3001844.
<https://doi.org/10.1371/journal.pbio.3001844>
PMID:[36342925](https://pubmed.ncbi.nlm.nih.gov/36342925/)
66. Mazzoleni S, Landi C, Carteni F, de Alteriis E, Giannino F, Paciello L, Parascandola P. A novel process-based model of microbial growth: self-inhibition in *Saccharomyces cerevisiae* aerobic fed-batch cultures. *Microb Cell Fact*. 2015; 14:109.
<https://doi.org/10.1186/s12934-015-0295-4>
PMID:[26223307](https://pubmed.ncbi.nlm.nih.gov/26223307/)
67. Mochida K, Nakatogawa H. Atg39 binding to the inner nuclear membrane triggers nuclear envelope deformation in piecemeal macronucleophagy. *Autophagy*. 2022; 18:3046–7.
<https://doi.org/10.1080/15548627.2022.2069957>
PMID:[35468041](https://pubmed.ncbi.nlm.nih.gov/35468041/)
68. Davey HM, Hexley P. Red but not dead? Membranes of stressed *Saccharomyces cerevisiae* are permeable to propidium iodide. *Environ Microbiol*. 2011; 13:163–71.
<https://doi.org/10.1111/j.1462-2920.2010.02317.x>
PMID:[21199254](https://pubmed.ncbi.nlm.nih.gov/21199254/)
69. Mijaljica D, Prescott M, Devenish RJ. A late form of nucleophagy in *Saccharomyces cerevisiae*. *PLoS One*. 2012; 7:e40013.
<https://doi.org/10.1371/journal.pone.0040013>
PMID:[22768199](https://pubmed.ncbi.nlm.nih.gov/22768199/)
70. Harari Y, Ram Y, Rappoport N, Hadany L, Kupiec M. Spontaneous Changes in Ploidy Are Common in Yeast. *Curr Biol*. 2018; 28:825–35.e4.
<https://doi.org/10.1016/j.cub.2018.01.062>
PMID:[29502947](https://pubmed.ncbi.nlm.nih.gov/29502947/)
71. Yofe I, Weill U, Meurer M, Chuartzman S, Zalckvar E, Goldman O, Ben-Dor S, Schütze C, Wiedemann N, Knop M, Khmelinskii A, Schuldiner M. One library to make them all: streamlining the creation of yeast libraries via a SWAp-Tag strategy. *Nat Methods*. 2016; 13:371–8.
<https://doi.org/10.1038/nmeth.3795>
PMID:[26928762](https://pubmed.ncbi.nlm.nih.gov/26928762/)
72. Firmenich AA, Elias-Arnanz M, Berg P. A novel allele of *Saccharomyces cerevisiae* RFA1 that is deficient in recombination and repair and suppressible by RAD52. *Mol Cell Biol*. 1995; 15:1620–31.
<https://doi.org/10.1128/MCB.15.3.1620>
PMID:[7862153](https://pubmed.ncbi.nlm.nih.gov/7862153/)
73. Jedrychowska M, Denkiewicz-Kruk M, Alabrudzinska M, Skoneczna A, Jonczyk P, Dmowski M, Fijalkowska IJ. Defects in the GINS complex increase the instability of repetitive sequences via a recombination-dependent mechanism. *PLoS Genet*. 2019; 15:e1008494.
<https://doi.org/10.1371/journal.pgen.1008494>
PMID:[31815930](https://pubmed.ncbi.nlm.nih.gov/31815930/)

SUPPLEMENTARY MATERIALS

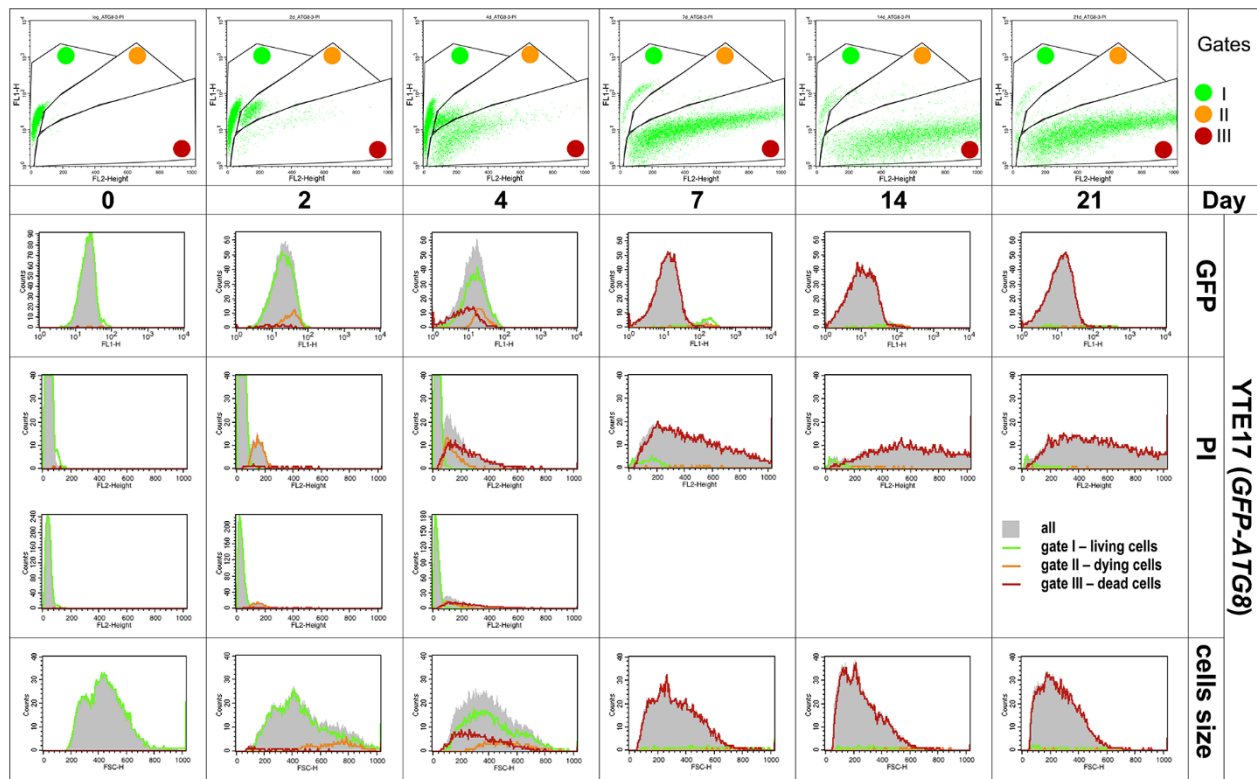
Supplementary Figures



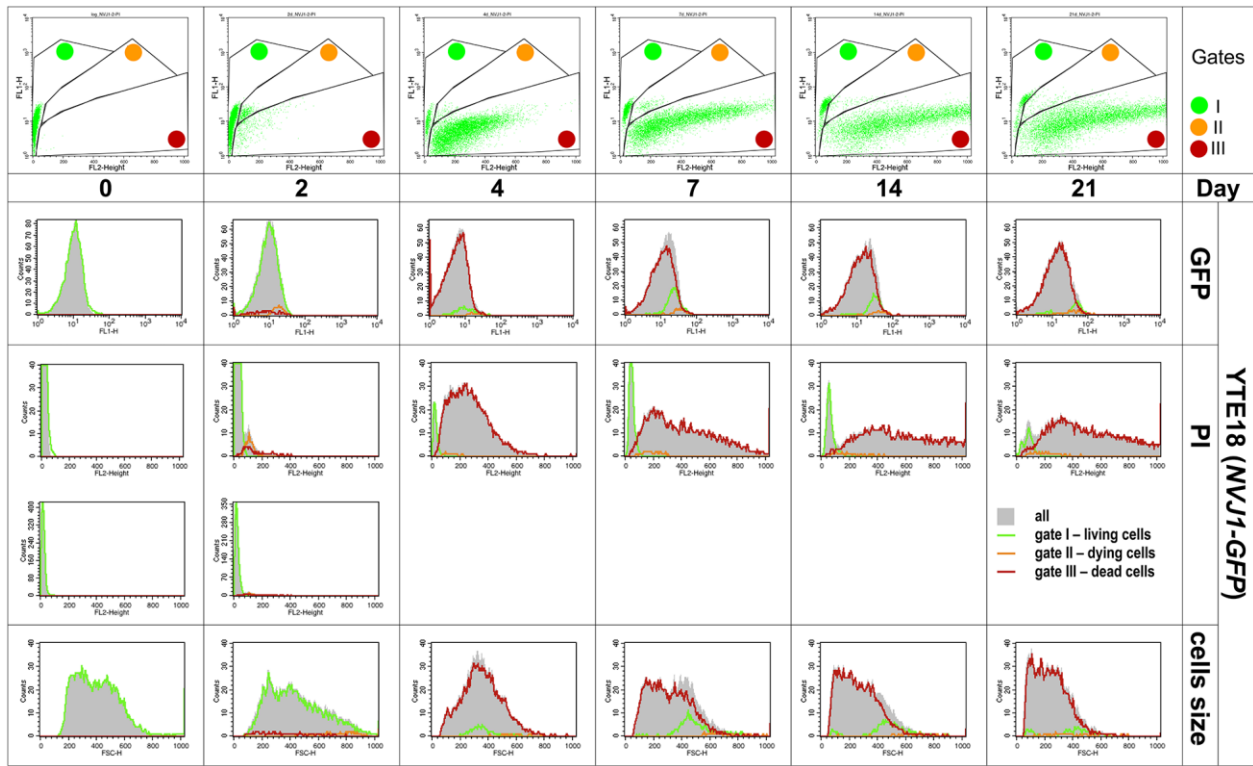
Supplementary Figure 1. DNA content and cells size of control cells cultivated in different type of medium to a given phase of growth. Gray, thin line – Haploid (BY4741); Black, thick line – Diploid (BY4743).



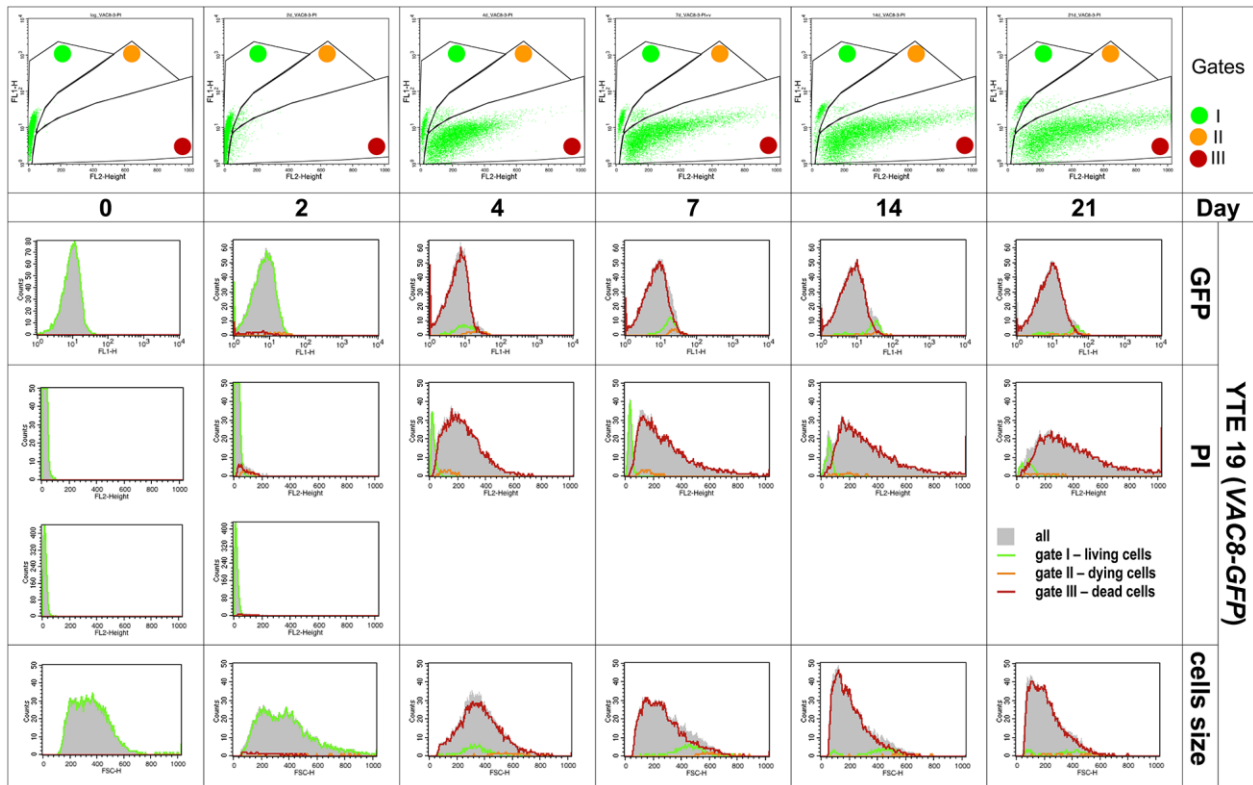
Supplementary Figure 2. Changes in the autophagy markers' localization during chronological aging. Microscopic analysis of strains carrying fluorescently tagged autophagy markers: (A) YTE17 (GFP-ATG8), (B) YTE20 (ATG39-GFP), (C) YTE18 (NVJ1-GFP), and (D) YTE19 (VAC8-GFP) in a given day of CLS experiment. Examples shown in (A–D) are focused on cells that were still viable at the analyzed time point. The microscopic images were collected and processed under the same conditions, so the differences in signal intensity are veritable. (E) Categories of counted phenotypes - examples.



Supplementary Figure 3. Changes in the GFP-Atg8 fluorescence and cell viability measured by flow cytometry during the CLS of YTE17 (GFP-ATG8). Cells in the population were divided into three subpopulations: living, dying, and dead, according to the presented fluorescence signal. The upper panel shows gating conditions. Lower panels show histograms for each channel and time point.



Supplementary Figure 4. Changes in the Nvj1-GFP fluorescence and cell viability measured by flow cytometry during the CLS of YTE18 (NVJ1-GFP). Cells in the population were divided into three subpopulations: living, dying, and dead, according to the presented fluorescence signal. The upper panel shows gating conditions. Lower panels show histograms for each channel and time point.



Supplementary Figure 5. Changes in the Vac8-GFP fluorescence and cell viability measured by flow cytometry during the CLS of YTE19 (VAC8-GFP). Cells in the population were divided into three subpopulations: living, dying, and dead, according to the presented fluorescence signal. The upper panel shows gating conditions. Lower panels show histograms for each channel and time point.

